

CO₂ EOR Performance Evaluation in Unconventional Reservoir using Huff'n'Puff Scheme

Master Thesis report

by

Saleh Alfaleh

to obtain the degree of Master of Science
at the Delft University of Technology

Thesis committee:

Chair: Prof.dr. P.L.J.Zitha

Supervisors: Dr. Denis Voskov
Dr. Anne Pluymakers

An electronic version of this thesis is available at <http://repository.tudelft.nl/>.

Acknowledgement

First, I would like to express my sincere gratitude to my thesis supervisor, Professor Pacelli Zitha. Your guidance, support and encouragement have been invaluable throughout the entire research process. I am deeply indebted to you for your patience, understanding, and willingness to share your expertise with me. I am fortunate to have you as my thesis supervisor.

I would also like to thank my thesis committee members, Dr. Denis Voskov and Dr. Anne Pluymakers, for your valuable feedback and suggestions. Your insights have helped me to improve my work significantly.

In addition, I would like to extend my gratitude to my colleagues and friends Dr. Jaber Aljaberi, Majed Alghamdi and Saleh AlAtwah for their support and encouragement. I am grateful for the opportunity to have learned from such a talented and dedicated group of individuals.

Finally, I would like to thank my parents, family and friends for their unwavering support throughout my academic journey. I could not have done this without you.

Abstract

The increasing global demand for energy has necessitated the exploration of untapped potential energy resources. Unconventional oil reservoirs present a significant opportunity for development through various enhanced oil recovery (EOR) methods. Among these methods, the huff'n'puff scheme using Carbon Dioxide (CO₂) EOR has emerged as a potent technique, considering both productivity and its impact on global warming. Unlike water injection, CO₂ EOR exhibits high injectivity potential in tight formations, making it a promising approach.

This thesis focuses on investigating the performance of CO₂ EOR in unconventional oil reservoirs using the huff'n'puff scheme through a comprehensive reservoir simulation study based on an open-source geological model. The study evaluates the effects of key parameters on oil production, including injection rate, injection time, soaking time, diffusion coefficient, and well completion.

The simulation results demonstrate that CO₂ EOR can effectively enhance oil recovery from unconventional oil reservoirs. Specifically, the study reveals that implementing CO₂ EOR increases cumulative oil production by 27% after 20 years compared to natural depletion cases. Furthermore, when incorporating a two-year primary recovery period, cumulative oil production is further elevated to 45%. By implementing the findings from the sensitivity study, cumulative oil production can be increased up to 67% in the optimum case.

In terms of the influence of the tested parameters on oil production, the study identifies that higher injection rates and longer injection, soaking, and production times for each cycle improve oil recovery until reaching an optimum value. Additionally, extending injection period by 10 times in each cycle with the same CO₂ injected volume improved cumulative oil production by 7% compared to fixed injection rate as a result of longer diffusion and dissolution time. Moreover, implementing bottom CO₂ injection targeting bottom layers improves vertical sweep efficiency due to buoyancy forces. The study also highlights the importance of the diffusion coefficient, as higher values facilitate faster CO₂ transport, resulting in higher oil recovery and reduced CO₂ reproduction.

This thesis provides valuable insights into the design and implementation of CO₂ EOR projects in tight oil reservoirs. It emphasizes the need for careful selection of optimal operating conditions based on specific reservoir properties and highlights the significance of the diffusion mechanism in CO₂ EOR performance. The findings contribute to the development of more effective CO₂ EOR strategies for unconventional oil reservoirs, addressing gaps in previous research. Moreover, the study's outcomes have practical implications for improving the design and implementation of CO₂ EOR projects in the field, ultimately leading to increased oil production.

Contents

List of Figures	v
List of Tables	vii
1 Introduction	1
1.1 CO ₂ EOR Background	1
1.2 Research Motivation	1
1.3 Problem Statement and Objective	1
1.4 Structure of the Thesis	2
2 Literature Review	3
2.1 CO ₂ EOR Mechanisms.	3
2.2 CO ₂ Miscibility	3
2.3 CO ₂ Molecular Diffusion	4
2.4 CO ₂ Injection Schemes	4
2.5 Supercritical CO ₂	6
2.6 CO ₂ Storage	6
2.7 Petrophysical Changes During CO ₂ Flooding.	6
2.8 Major Challenges.	7
2.9 Field Scale Pilot Tests	8
3 Geological Model	9
3.1 COSTA Model	9
3.2 Geological Background	9
3.3 Data Used	9
3.4 Sector Model	10
3.5 Sector Model Modifications	11
4 Reservoir Simulation	14
4.1 Sector Model	14
4.2 Dynamic Reservoir Properties	14
5 Assessment of CO₂ EOR Performance	18
5.1 Base Case	18
5.2 Sensitivity Study	25
5.3 Optimum Case	42
6 Conclusions	44
7 Recommendations	45
References	48

Nomenclature

List of Abbreviations

ACW	Active Carbonated Water	a_g	Gas endpoint relative permeability
ACWAG	Active Carbonated Water-Alternating Gas	b_g	Exponential factor
ACWI	Active Carbonated Water Injection	CO_2	Carbon Dioxide
API	American Petroleum Institute	K	Kalvin
CW	Carbonated Water	k	Permeability
CWI	Carbonated Water Injection	k_h	Horizontal permeability
EOR	Enhanced Oil Recovery	k_{rg}	Gas relative permeability
EOS	Equation of State	k_{rog}	Oil relative permeability
FCM	First Contact Miscibility	k_v	Vertical permeability
FWL	Free Water Level	m	Meter
GOR	Gas-Oil Ratio	m^2/d	Square meter per day
IFT	Interfacial Tension	mD	milliDarcy
MCM	Multiple Contact Miscibility	mm^3	Thousand cubic meter
MICP	Mercury Injection Capillary Pressure	mm^3/d	Thousand cubic meter per day
MMP	Minimum Miscibility Pressure	Mpa	Mega Pascal
RBA	Rising-Bubble Apparatus	n_{pg}	Angular velocity
RRT	Reservoir Rock Type	p_{cog}	Gas-oil system capillary pressure
SACROC	Scurry Area Canyon Reef Operations Committee	$p_{CS_{lc}}$	Capillary pressure at critical liquid saturation
U.A.E	United Arab Emirates	s_{gc}	Residual gas saturation
VIT	Vanishing Interfacial Tension	s_g	Gas saturation
WAG	Water-Alternating Gas	s_{lc}	Critical liquid saturation
WI	Water Injection	s_{org}	Angle of attack
		s_{or}	Residual oil saturation
		s_o	Oil saturation
		s_{wc}	Connate water saturation

List of Symbols

$^{\circ}C$ Degree Celsius

List of Figures

2.1	Diagram of CO ₂ Huff'n'Puff injection scheme [23]	5
3.1	Lithostratigraphic column of Rub AlKhali basin [34]	9
3.2	COSTA sector model	10
3.3	Selected sector model for dynamic simulation	11
3.4	Sector model porosity and permeability histogram	11
3.5	Selected sector model after permeability multiplier	12
3.6	Sector model permeability histogram with 0.01 K multiplier	12
3.7	Selected sector model after grid refinement	13
4.1	Gas relative permeability curve versus gas saturation	15
4.2	Oil relative permeability curve versus oil saturation	16
4.3	Capillary pressure versus gas saturation	16
5.1	Simulation Results of base case	19
5.2	Cumulative oil production of base case and natural depletion case	20
5.3	Cumulative oil production with primary recovery period	20
5.4	Pressure map from initial time until first injection cycle	21
5.5	Gas saturation map after first injection period	21
5.6	Gas saturation map after first soaking period	22
5.7	Pressure profile in huff'n'puff cycles	22
5.8	Pressure map before and after soaking	23
5.9	Production gas-oil ratio plot	24
5.10	Gas saturation map after first EOR production period	24
5.11	Cumulative gas injection and production	25
5.12	Cumulative oil production plots at different injection rates	26
5.13	Cumulative oil production at different injection rates	26
5.14	Cumulative gas production at different injection rates	27
5.15	Cumulative oil production plots at different injection durations	28
5.16	Cumulative oil production at different injection durations	28
5.17	Gas saturation cross section map after first injection cycle	29
5.18	Incremental oil gain per day for the additional lifetime needed	29
5.19	Cumulative oil production plots at different injection durations with fixed volume	30
5.20	Cumulative oil production at different injection durations with fixed volume	30
5.21	Cumulative gas production plots at different injection durations with fixed volume	31
5.22	Cumulative oil production plots at different soaking periods	32
5.23	Cumulative oil production at different soaking periods	32
5.24	Cumulative gas production plots at different soaking periods	33
5.25	Gas saturation cross section map for 120 days soaking time case	33
5.26	Incremental oil gain per day for the additional lifetime needed	33
5.27	Cumulative oil production plots at different production periods	34
5.28	Cumulative oil production at different production periods	35
5.29	Cumulative oil production plots at different incremental injection rate cases	36
5.30	Cumulative oil production at different incremental injection rate cases	36
5.31	Reservoir pressure plots for different incremental injection rate cases	37
5.32	Gas saturation cross section map comparison between case 1 and 6	37
5.33	Cumulative oil production plots at different diffusion coefficients	38
5.34	Cumulative oil and gas production at different diffusion coefficients	38
5.35	Gas saturation cross section map for different diffusion coefficient cases	39

5.36 Cumulative oil production plots at different well completion cases 40
5.37 Cumulative oil production at different well completion cases 40
5.38 Cumulative gas injection plots at different well completion cases 41
5.39 Gas saturation cross section map of different well completion cases 42
5.40 Oil production rates at different well completion cases during primary recovery 42
5.41 Simulation results of optimum case 43

List of Tables

3.1	Model parameters for optimum case	13
4.1	Model size comparison with literature	14
4.2	Reservoir crude oil compositional data for the Peng–Robinson EOS [12]	17
4.3	Binary interaction parameters for oil components [12]	17
5.1	Model input parameters for base case	18
5.2	Different injection cases at fixed injection volume	30
5.3	Production time and number of cycles cases at a fixed project lifetime	34
5.4	Different cases of incremental injection rates	36
5.5	Different cases of well completion	39
5.6	Model parameters for optimum case	43
5.7	Injection rates sequence	43

Introduction

1.1. CO₂ EOR Background

The use of carbon dioxide (CO₂) to enhance oil recovery in oil reservoirs is not a new topic. According to [1], CO₂ flooding for EOR approach started in 1930s with experimental and laboratory studies until the first field scale application of CO₂ EOR in 1972 at Scurry Area Canyon Reef Operations Committee (SACROC) unit of Permian Basin. Over the past four decades, CO₂ EOR experienced an immense success in conventional oil reservoirs [2]. After CO₂ EOR had proven its influence on oil recovery in conventional reservoirs, a focus has been directed towards understanding CO₂ EOR potential in unconventional oil reservoirs over the past decade [3]. The development of unconventional reservoirs uses infill drilling and multistage fracturing as a current practice for short-term oil gain, which only enhances recovery by 10% over primary recovery [4][5]. The use of water injection as a mean for enhancing recovery in tight reservoirs did not result in significant oil gain. According to [6], the increase in oil recovery in tight reservoir after water injection is less than 10%, with a significant oil production reduction post water breakthrough. There are several factors that limit oil gain when water flooding is utilized in tight formations. One is the low injectivity of tight formations due to low permeability that leads to low water injection rates [7]. Another issue is the water fingering in tight reservoirs due to the difference in viscosity between injected water and reservoir oil [7]. In addition, water can lead to swelling of clay minerals that can create a damaged zone and reduction in permeability in some reservoirs [8]. On the other hand, CO₂ flooding is easier to inject and would not lead to noticeable formation damage resulting in higher oil recovery [5][9]. This makes CO₂ flooding a more attractive approach to be utilized for enhancing oil recovery in unconventional reservoirs.

1.2. Research Motivation

There is a continuous demand on energy supply worldwide, and this demand is increasing with time due to world population increase. According to [10], fossil fuel will be the dominant energy source until 2050 even with the current energy transition. Unconventional oil reservoirs holds great untapped potential that can be unveiled with the implementation of a well designed EOR method. The use of CO₂ as EOR method in tight oil reservoirs not only improves recovery, but also aids in reducing CO₂ emissions. The industrial revolution over the past decades increased CO₂ emissions and there is a great need to capture these emissions to avoid global warming [1]. Therefore, utilizing CO₂ for EOR would maintain the world energy supply while storing CO₂ in the subsurface. In fact, CO₂ is considered one of the most potent EOR methods when accounting for global warming [11]. The research aims to evaluate CO₂ EOR in unconventional oil reservoirs using huff'n'puff scheme. The selection of the huff'n'puff scheme is mainly due to the advantages it holds in terms of short-term oil gain and low economic cost. The use of a single well for CO₂ injection and oil production leads to a lower project capital cost. Even though the topic has been discussed in several studies in the literature, there is few areas of gap and other areas that show contradiction. This study will shed more light on these gaps and provide a detailed assessment on the points of contradiction in previous studies.

1.3. Problem Statement and Objective

There are many factors that affect CO₂ EOR performance in unconventional oil reservoirs using huff'n'puff scheme. Previous studies on the topic using numerical modeling covered several parameters including

injection rate, injection time, soaking time and diffusion coefficient. However, these factors were not deeply investigated with gaps to be filled in order to enhance oil production. Therefore, the objective of this thesis is to understand the influence of the controlling factors on CO₂ EOR performance in unconventional oil reservoirs using huff'n'puff scheme through reservoir simulation. This includes the evaluation of the previously studied parameters to verify findings along with the assessment of new parameters that can enhance oil production.

1.4. Structure of the Thesis

This thesis includes a total of six chapters. Chapter 1 is the current chapter and it provides a brief background on CO₂ EOR and the motivation behind choosing this research topic along with problem statement and objectives. Then, Chapter 2 shares a literature review from previous studies on CO₂ EOR in unconventional reservoirs. It includes the findings on main CO₂ EOR mechanisms, different injection schemes, major challenges and field scale applications. After that, Chapter 3 describes the chosen geological model and the implemented modifications to meet the objectives of the numerical simulation study. Then, Chapter 4 presents the simulation software and dynamic properties used as input parameter for reservoir simulation. Moreover, Chapter 5 presents a detailed evaluation of CO₂ EOR in tight reservoir using huff'n'puff scheme based on simulation results. A sensitivity study is performed on several parameters influencing CO₂ EOR performance in terms of oil recovery. Based on findings and conclusions from the sensitivity study, an optimum CO₂ EOR is presented and discussed. Finally, Chapter 6 summarises the major findings from this thesis and Chapter 7 provides recommendations for future work.

Literature Review

2.1. CO₂ EOR Mechanisms

There are several mechanisms that take place in the subsurface hydrocarbon reservoirs during CO₂ enhanced recovery. According to [10], there are four main mechanisms: Interfacial tension (IFT) reduction, oil swelling, oil viscosity reduction and light component extraction. During CO₂ injection, CO₂ will dissolve in reservoir crude oil leading to these different mechanisms. The dissolution of CO₂ in crude oil will firstly lead to oil swelling and viscosity reduction that will improve the mobility of the mixture resulting in higher oil recovery. The rate of dissolution is dependent on CO₂ injection pressure, and higher pressures will result in higher dissolution leading to an improvement in oil recovery and sweep efficiency [11]. Moreover, a reduction in interfacial tension between CO₂ and crude oil will occur resulting in a more homogeneous mixture reducing the residual oil and improving fluid displacement leading to higher oil recovery. The degree of IFT reduction will depend on fluid miscibility, which will be discussed in the next section. The dissolved CO₂ in oil would also lead to the extraction of lighter oil component in the reservoir. Density of injection CO₂ would control the hydrocarbons extraction process, where CO₂ will extract more and heavier hydrocarbon components at higher CO₂ densities [12]. [13] included two more EOR mechanisms: alternation of wettability and relative permeability and an increase in reservoir pressure. Wettability is defined as the degree of adhesion of a fluid to rock surface when other immiscible fluids are present, and it can be measured by the contact angle between fluid to rock surface [14]. The alternation in wettability towards water-wet will lead to reduction in residual oil leading to higher oil recovery. All of the mentioned mechanisms during CO₂ EOR process are acting to improve crude oil recovery.

2.2. CO₂ Miscibility

Fluid miscibility is considered one of the key mechanisms that can take place during CO₂ EOR. Miscibility is defined as the formation of a homogeneous mixture through the mixing of different substances due to a reduction in their IFT [15]. For CO₂ injection in a hydrocarbon reservoir, miscibility can be established as either first contact miscibility (FCM) or multiple contact miscibility (MCM) [16]. In FCM, injected gas can mix directly with crude oil under reservoir condition [16]. On the other hand, MCM is achieved through continuous contacts between injected CO₂ and crude oil reducing IFT gradually while continuous CO₂ dissolution in oil is taking place until reaching complete miscibility [16]. In the case of CO₂ injection in crude oil reservoir, the process would be a multiple contact miscibility (MCM) [17][16]. To achieve CO₂ miscibility with crude oil, crude oil must have sufficient amount of light components to be extracted by CO₂ to achieve complete miscibility [16]. In addition, the operating subsurface pressure during CO₂ injection has to exceed a limit called minimum miscibility pressure (MMP). This is defined as the minimum operating pressure that would result in CO₂ dynamic or MCM with crude oil [17]. Otherwise, CO₂ flooding will be immiscible. MMP can be measured in the lab using different tools and techniques such as slim-tube test, Rising-bubble apparatus (RBA) and Vanishing interfacial tension (VIT) technique [17]. MMP is highly dependent on crude oil molecular weight and chemical composition [17].

In immiscible CO₂ flooding, the main oil recovery mechanisms are oil viscosity reduction, oil swelling, IFT reduction and immiscible displacement [17]. However, viscous fingering and gas channeling are disadvantages observed in immiscible technique and can lead to low sweep efficiency [18]. Moreover,

gravity plays a role in influencing the displacement of CO₂, where top gas injection leads to better performance compared to bottom injection [19]. Gravity effect is directly related to reservoir thickness, but it can be minimized at high CO₂ injection rates [19]. As for miscible CO₂ flooding, it has the same oil recovery mechanisms as immiscible flooding with the addition of diminishing IFT by reducing the density difference due to pressure increase above MMP [1]. In this technique, most light components in the crude oil are extracted by CO₂, and oil-CO₂ interface almost disappears to form a single phase flow which can easily flow in porous medium [19]. Unlike immiscible technique, viscous fingering and early gas breakthrough are eliminated during miscible flooding [16]. In addition, gravity doesn't have an important role in miscible flooding [19]. For unconventional reservoirs, majority of previous studies recommended miscible gas EOR [3]. According to [19], highest oil recovery and CO₂ storage potential is achieved during miscible flooding. Moreover, coreflood experiments resulted in an average recovery of 90% following a miscible CO₂ flooding illustrating the high efficiency in oil recovery enhancement in tight formation [6]. Lastly, [17] observed that after CO₂ breakthrough, oil recovery increases slightly in immiscible flooding but significantly in miscible flooding as a result of strong light hydrocarbon extraction by CO₂ and miscible displacement.

2.3. CO₂ Molecular Diffusion

Molecular diffusion is considered a key mechanism in CO₂ EOR process in shale oil reservoirs [20][3]. Molecular diffusion is defined as the movement of molecules due to a difference in concentration gradient in a mixture of fluids [20]. For CO₂ injection in crude oil reservoir, the injected CO₂ molecules diffuse into the oil moving from high concentration of CO₂ into low concentration of CO₂ in oil. According to [4], performance of CO₂ huff-n-puff pilot tests were not meeting expectations due to the inaccurate prediction of CO₂ diffusion mechanism in these reservoirs. Based on several literature reports, the significance of molecular diffusion mechanism on CO₂ EOR performance is dependent on injection scheme and reservoir type. According to [4], molecular diffusion mechanism is significant in huff-n-puff injection scheme but not in continuous gas injection. As for reservoir type, the effect of CO₂ diffusion mechanism on EOR process in conventional reservoirs is almost non-existence based on experimental studies [3]. This is because of the higher permeability in conventional reservoirs resulting in a dominant advective flow due to pressure gradient. To incorporate CO₂ molecular diffusion in a scientific research or field development, CO₂ diffusivity rate has to be evaluated. Identification of CO₂ diffusivity rate is a key factor in the success of CO₂ EOR in shale oil reservoirs [4]. This is highly important in numerical simulations as neglecting or inaccurately identifying diffusion rate might result in underestimation or overestimation of oil recovery during CO₂ EOR [20]. In a low CO₂ molecular diffusivity cases, exposure time and contact area between injected CO₂ and reservoir oil need to be substantially increased for better EOR performance [3]. There are several parameters that can influence CO₂ diffusion coefficient in an oil reservoir. [21] study concluded that reservoir pressure, temperature and oil composition would impact CO₂ diffusion coefficient. Higher reservoir pressure and temperature with lighter crude oil leads to higher CO₂ diffusion coefficient.

2.4. CO₂ Injection Schemes

CO₂ Huff'n'Puff Scheme

The CO₂ huff'n'puff scheme is one of the schemes used for CO₂ EOR. It follows a cyclic process utilizing a single well, where each cycle starts with CO₂ injection followed by a soaking period and ends with production as shown in figure 2.1. First CO₂ EOR huff'n'puff project was conducted in Trinidad and Tobago for conventional reservoirs in 1984 [3]. This scheme has been implemented successfully since then in conventional reservoirs showing to be most effective for short term EOR, and it can be designed for tight reservoirs as well [13]. In tight reservoirs, EOR mechanism depends on CO₂ diffusion, viscosity reduction and dissolution drive [10]. Soaking period within each cycle provides time for CO₂ diffusion and dissolution in oil reducing its viscosity [13]. Based on lab experiments conducted on fractured plugs, this scheme had a better performance compared to continuous CO₂ flooding [2]. One disadvantage of this scheme is that most of the injected CO₂ will be reproduced [5]. There are also challenges that need to be addressed and evaluated when studying CO₂ huff'n'puff. One challenge is the drainage area that can be covered and swept from a single well. This is controlled by the reservoir permeability and CO₂ ability to spread during injection and soaking times. After several cycles, the performance of huff'n'puff significantly drops due to the reduction of oil saturation near well, and more CO₂ needs to be injected to maintain production [13][22]. Another challenge is the CO₂ utilization aspect and the control of CO₂ reproduction. These challenges can

also be linked to the soaking period as it can influence both oil recovery and CO₂ utilization. However, previous research on soaking period effect is not aligned in order to overcome these challenges. According to one study conducted by [13], soaking time doesn't have much impact on oil recovery. Another experiment indicated that soaking time is needed to yield the highest oil recovery regardless of the soaking time used [13]. A third research found that soaking time is needed and there is an optimum soaking time of 1 month to achieve the highest oil recovery [22]. Therefore, a more in-depth analysis of the soaking time influence on not only oil recovery, but also CO₂ utilization is needed for better implementation of CO₂ huff'n'puff scheme.

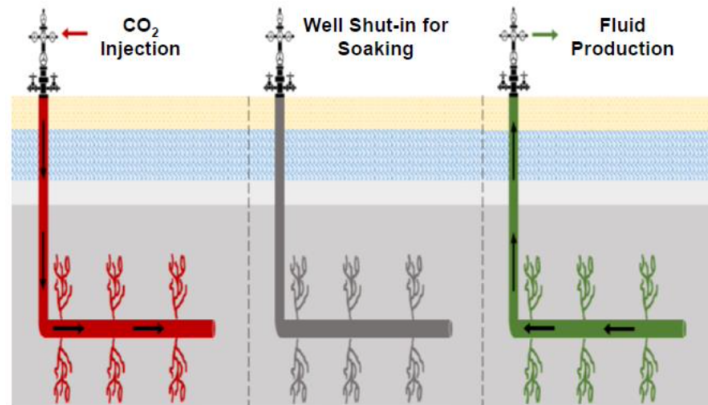


Figure 2.1: Diagram of CO₂ Huff'n'Puff injection scheme [23]

2.4.1. Other Injection Schemes

There are several other CO₂ EOR injection schemes that were evaluated and tested through lab experiments, numerical simulation and field applications. The following list includes eight different CO₂ injection schemes: (1) Continuous CO₂ flooding, (2) CO₂ flooding coupled with soaking period, (3) Water-alternate CO₂ injection (WAG), (4) CO₂ injection with chased WI, (5) Carbonated water injection (CWI), (6) Carbonated water-alternating gas injection, (7) Active carbonated water injection (ACWI), (8) Active carbonated water-alternating gas (ACWAG). These schemes will not only differ in their resulting oil recovery, but also CO₂ utilization [24]. Starting with continuous CO₂ flooding, it consists of both injection and production wells that can be placed with different patterns. One advantage this scheme holds is the higher CO₂ storage [10]. However, it results in low displacement efficiency and gas channeling leading to early CO₂ breakthrough, which is considered a major disadvantage for this scheme [11]. This scheme can be modified by including a shut-in period after injection, and it would be called CO₂ flooding coupled with soaking period. Results showed that this modification leads to higher oil recovery due to the given time for CO₂ to transport and further dissolve in oil while reacting with formation to increase its permeability [7].

Other schemes have included water in the CO₂ EOR process in order to improve oil recovery. Starting with WAG scheme, the use of water results in a delayed gas breakthrough and a control in mobility avoiding CO₂ fingering and an improved sweep and displacement efficiency based on several field applications [10][6]. However, CO₂ WAG is less effective in high heterogeneity formations, as it recovers residual oil in high permeability zones [18]. Rather than having an alternating injection, CO₂ injection chased with WI scheme can be followed. Based on a numerical study comparing the two schemes, CO₂ injection chased with WI is considered the better option because of the resulting incremental oil and CO₂ utilization [24]. After that, a new approach evolved by using carbonated water (CW) instead, where CO₂ is mixed with water before injection to have higher viscosity and lower mobility for an enhanced volumetric sweep efficiency [1]. After injection of carbonated water, CO₂ transports from formation water to reservoir oil due to the solubility of CO₂ in oil [6]. The acidic behaviour would also lead to a reduction in interfacial tension and alteration in wettability to a more favourable water-wet system [1]. From coreflood experiments, CWI had a better performance compared to WAG utilizing similar CO₂ amount during injection [6]. Another approach is to utilize CW in a WAG scheme. According to a comparison study between different CO₂ flooding schemes, carbonated water alternating gas injection yielded the highest oil recovery [5]. Other than

formation water and carbonated water, a new scheme is developed by adding surfactant on CW to become active carbonated water (ACW). The advantage of including surfactant is to reduce interfacial tension significantly in addition to wettability alteration [6]. An experiment conducted by [6] showed that ACW if used as direct injection or as a WAG approach would lead to higher oil recovery compared to previous methods. Nevertheless, the use of CW or ACW might impose several challenges such as corrosion when implemented at a field scale, since conducted studies on this topic is mainly based on lab experiments and numerical simulation.

2.5. Supercritical CO₂

The utilization of CO₂ in its supercritical condition for EOR in conventional and unconventional reservoirs has been investigated in several researches. Supercritical CO₂ has different fluid properties compared to its gaseous phase, where it maintains the characteristics of a gas and the density of a liquid [1][25]. It also has a near gas viscosity and high diffusion coefficient [25]. Supercritical would also maintain a good injectivity in tight reservoirs [26]. CO₂ will reach its supercritical condition once the temperature exceeds 31.26° C and the pressure exceeds 7.4 Mpa [8].

2.6. CO₂ Storage

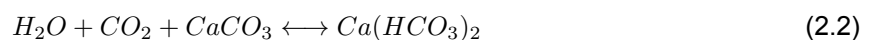
Research and field applications of CO₂ storage in subsurface reservoirs have been of great interest in the past decade in order to reduce CO₂ emissions to avoid global warming. As part of CO₂ EOR, CO₂ storage will also occur indirectly in the subsurface by replacing the produced oil. In general, there are four main CO₂ storage mechanisms: stratigraphic trapping, solubility trapping, capillary trapping and mineral trapping [10]. For CO₂ EOR in tight formations, the dominating storage mechanisms are solubility trapping and capillary trapping [10]. Different CO₂ injection schemes can result in different sequestration ratio and volume. In a numerical simulation study performed by [10], results showed that continuous injection scheme leads to a higher CO₂ storage volume by 15% compared to WAG scheme, mainly because continuous injection scheme uses a much larger CO₂ during injection. The study also observed that water injection rate in WAG scheme would negatively influence CO₂ storage. To evaluate storage in another scheme, [6] performed a coreflood experiment using carbonated water injection (CWI) scheme to identify 46% stored CO₂ volume, highlighting the storage potential this scheme offers. The storage potential during the use of supercritical CO₂ was also investigated in long-core experiments done by [26] showing effective CO₂ storage results. The same study also showed that another factor that can influence the sequestration volume is CO₂ breakthrough time. Results showed that gas breakthrough can negatively impact CO₂ storage. 85% of injected CO₂ was stored before breakthrough and reduced to 38-46% post breakthrough at its final stage. The study also evaluated the impact of reservoir permeability and stated that lower permeability would lead to higher CO₂ storage volume.

2.7. Petrophysical Changes During CO₂ Flooding

When CO₂ is injected in a subsurface reservoir, the formation petrophysical properties can be impacted through multiple chemical reactions. Some studies showed that CO₂ injection can negatively impact reservoir petrophysical properties, while others observed enhancement in reservoir porosity and permeability [14]. One chemical reaction that occurs is the one between injected CO₂ and formation water shown in the following chemical formula [27]:



In this reaction, the formed carbonic acid as a result of CO₂ dissolution in brine can dissolve parts of dolomite, calcite and feldspar in the rock resulting in new micro and nanopores [27]. This is represented through the following chemical reaction [24]:



The carbonic acid reaction with calcite results in the the formation of calcium bicarbonate. A large number

of research results show that injected CO₂ into formation during CO₂ flooding will dissolve in the formation water to produce carbonate precipitation [28]. Therefore, mineral dissolution increases porosity and permeability through dissolution of minerals, but resulting secondary precipitation decreases porosity and permeability [29][24]. According to a numerical study, large amount of precipitation occurs near bottom of the well as a result of large pressure difference near production well [28]. Accounting for these chemical reactions in numerical modeling can also have a noticeable impact on oil recovery prediction. A simulation study performed by [28] showed that after 20 years of production, ultimate recovery drops from 37.64% to 33.45% after including precipitation. Therefore, CO₂ injection impact on reservoir petrophysical properties should be considered in numerical models to have more representative results.

2.8. Major Challenges

There are many challenges that can be encountered during the development of CO₂ EOR project. These challenges can greatly influence the outcome and performance of any CO₂ flooding project in terms of enhanced recovery. The main challenges that will be covered and discussed in this section are sweep efficiency, presence of fractures and asphaltene precipitation.

2.8.1. Sweep Efficiency

The low areal and vertical sweep efficiency during CO₂ flooding is a major challenge, especially in tight reservoirs [10]. Reservoir heterogeneity has a significant impact on horizontal and vertical sweep efficiency that can lead to gas channeling in high conductive pathways [30]. Gas channeling would result in early CO₂ breakthrough time which will negatively impact areal sweep efficiency and oil recovery. Viscous fingering is another behaviour that can occur in oil reservoirs during the injection of CO₂, leading to significant amount of bypassed oil [10]. This is due to the difference in viscosities between injected CO₂ and crude oil, where CO₂ viscosity is much lower resulting in unfavorable mobility ratio [13]. In addition to reservoir heterogeneity, buoyancy-driven forces have also an impact on vertical sweep efficiency. According to [10], CO₂ buoyancy-driven forces would lead to lower vertical sweep efficiency with highest sweep at top layer. Several studies investigated methods to overcome gas channeling challenge in order to improve sweep efficiency and enhance oil recovery. There are common methods in controlling gas channeling: Blocking agent injection, WAG flooding and Foam flooding [18]. The use of blocking agents aims to block-off high conductive pathways such as high permeability zones or natural fractures to have a higher swept volume in order to enhance oil recovery [18].

2.8.2. Presence of Fractures

There are two different types of fractures that can be present in unconventional reservoirs: natural fractures and induced fractures. Starting with natural fractures, it frequently exists as a network creating high conductive pathways for fluid flow. Many researches have investigated the influence of natural fractures on CO₂ EOR in unconventional reservoirs. According to [20], intensity of natural fractures is a key factor that controls the success of CO₂ EOR in shale oil reservoirs. Natural fracture network is a main characteristic of unconventional reservoirs, and it can result in gas channeling and early gas breakthrough lowering sweep efficiency and oil recovery in CO₂ EOR projects [10][2][18][13]. On the other hand, other researchers stated that highly intensive natural fractures can enhance diffusivity of CO₂ leading to higher oil recovery [31][4].

As for induced fractures, it can be created around a drilled wellbore due to either high injection pressure above formation fracture gradient or thermal fractures due to temperature difference during injection. These induced fractures will have the same influence as the natural fractures in terms of offering high conductive pathways for fluid flow, which can be undesired in some cases. A field pilot test in Abu Dhabi evaluated the importance of surface heating of CO₂ prior to injection to avoid thermofrac [32]. It concluded that CO₂ will heat significantly during injection leading to minor temperature difference across sand face which will not create thermofrac.

2.8.3. Asphaltene Precipitation

Another highlighted challenge in the literature during injection of CO₂ in tight oil reservoir is the formation of asphaltene precipitation. It is defined as an insoluble material that can lead to formation damage, reduction in reservoir permeability and wettability alteration when precipitated [17]. Asphaltene precipitation can

form as a result of injected CO₂ interaction with reservoir crude oil [27]. The main reason for asphaltene precipitation during CO₂ injection is CO₂ solubility in crude oil [33]. A study by [33] found that asphaltene precipitation has a higher likelihood of occurring in light oil compared to heavy oil. Moreover, the study concluded that the precipitation is directly related to injection pressure and volume because it would lead to higher CO₂ dissolution. Another study conducted by [24] through a coreflood experiment to understand asphaltene precipitation during CO₂ flooding showed that asphaltene started to precipitate when CO₂ concentration reached to 29%. Thus, it has been concluded that asphaltene precipitation is directly proportional to CO₂ concentration.

The performance of CO₂ EOR project will be impacted by asphaltene precipitation due to resulting formation damage and reduction in permeability [7]. Therefore, actions have to be taken to overcome this challenge. One solution that has been implemented in a field trial test in Abu Dhabi is the injection of inhibitors to avoid any asphaltene deposition [32]. Continuous monitoring of asphaltene precipitation is highly important to ensure CO₂ injection rate is maintained to have the best CO₂ EOR performance.

2.9. Field Scale Pilot Tests

Several pilots tests were conducted at field scale to identify the potential of CO₂ EOR projects in tight reservoirs before full field implementation. In this section, a number of pilot tests will be discussed with their major findings. Starting with a pilot test conducted in Jilin oilfield in China in 2008, CO₂ EOR followed a continuous flooding scheme with a reversed 7-spot patten [16]. The injection pressure was above MMP aiming for miscible flooding technique. Results showed that due to low permeability, pressure could not propagate from injector to producer resulting in large area near the producer with immiscible flooding. Also, early CO₂ breakthrough observed was attributed to short well distance and presence of natural fractures. Another pilot test conducted in Bakken formation in North Dakota and Montana in 2008 and 2009, following a huff'n'puff scheme under miscible conditions [4]. Results did not show any clear oil increment under CO₂ EOR, although there was no reported injectivity issue. The disappointing results of huff'n'puff EOR was attributed to possible difference between proposed CO₂ diffusion mechanism in lab conditions and field conditions.

Moving to another pilot test in Abu Dhabi in 2009 utilizing continuous flooding scheme under miscible conditions [24]. During the pilot test, data were collected using logging and coring showing evidence of very low oil residual oil saturation. This proves the effectiveness of miscible displacement in enhancing oil recovery. The pilot did not experience any injectivity issues nor reservoir damage during the test. However, once CO₂ concentration increased in reservoir fluid to 29%, a tendency of asphaltene deposition is observed. Therefore, it was concluded that CO₂ concentration and asphaltene deposition are directly related. Another pilot test was conducted in Elm Coulee Area in Montana in 2009 utilizing CO₂ huff'n'puff scheme [3]. After injection and soaking, the well produced naturally for only 38 days. After which, it was put on a pump to restore production where rate increased reaching a peak followed by a continuous decline until end of test. Around half of the injected CO₂ volume in the first year was reproduced. There is an uncertainty when it comes to the increase in rate post injection in this test if it is attributed to CO₂ injection or the artificial pump. The discussed pilot tests does not capture all CO₂ EOR pilot tests in tight reservoirs, as there are many other pilots conducted in recent years available in the literature.

Geological Model

3.1. COSTA Model

In order to study CO₂ EOR process using huff'n'puff approach, a realistic geological model is needed. Unfortunately, there is a lack of detailed open-source geological models that would represent realistic geological features. Majority of these open-source models available are fully synthesized models that can include many uncertainties when used for numerical modeling. A recently developed open-source carbonate reservoir model called COSTA model [34] is chosen for this study. This geological model can be used to study CO₂ EOR and storage projects. COSTA model is a considered semi-synthetic but geologically realistic model since it is based on mixture of real and synthesized data. The model does not include any faults or fractures. The model consists of 1.3 million active grid cells, where each grid cell has a size of 250 m x 250 m with a thickness varying from 0.2 to 2 m. The model is roughly 50 m thick subdivided into 62 geological layers.

3.2. Geological Background

The Geological setting of COSTA carbonate model is in the Upper KharaiB Member (Early Cretaceous) in Rub Al Khali basin, which is a sub-basin of the wider Arabian Basin. Figure 3.1 presents the lithostratigraphic column of Rub AlKhali basin across multiple countries in the Middle East. Within the U.A.E. alone, this geological formation is referred to as both the Upper KharaiB Member and Thamama Zone B and is estimated to cover an area of 36,000 km². It is located in the north-eastern part of the Rub Al Khali basin. In terms of geological structure, Upper KharaiB Member geological structure consists of 3 main anticlines. The Upper KharaiB Member is roughly 50 m thick, and its thickness remains relatively constant. It is subdivided into two main units: B-Upper and B-Lower. The upper unit is made of grainy facies with higher rock permeability, while lower unit is made of Packstone/Wackestone facies with lower rock permeability.

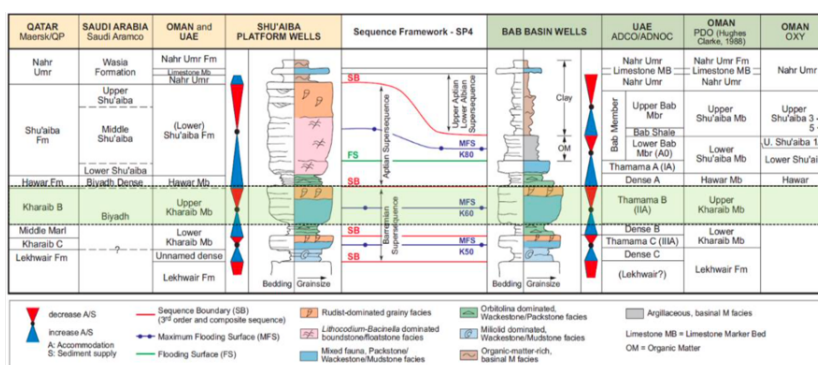


Figure 3.1: Lithostratigraphic column of Rub AlKhali basin [34]

3.3. Data Used

The dataset to build COSTA model uses 43 wells from fully anonymized published data from the north-eastern part of the Rub Al Khali basin. The dataset is a mixture of real and synthetic data from 22 fields in

U.A.E used as an analogue. Gathered well data such as real wireline logs and core data are used. To generate COSTA model, Upper Kharaib Member area in Rub Al Khali Basin had to be downsized from 36,000 km² down to 8,300 km². Thus, the downsized model would result in an area of 124 x 67 km size with 11 million grid blocks. The original well locations of all 43 wells were rescaled proportionally by a factor of four to decrease the areal coverage from 36,000 km² down to 8,300 km². After that, COSTA model is subdivided into three individual anticline structures. Each geological closure will act as a different reservoir. Thus, a sector model of the full COSTA model containing 17 wells out of 43 in one anticline with a size of 60 km x 26 km is shared as an open-source sector model. A 3D view of COSTA sector model is shown in figure 3.2.

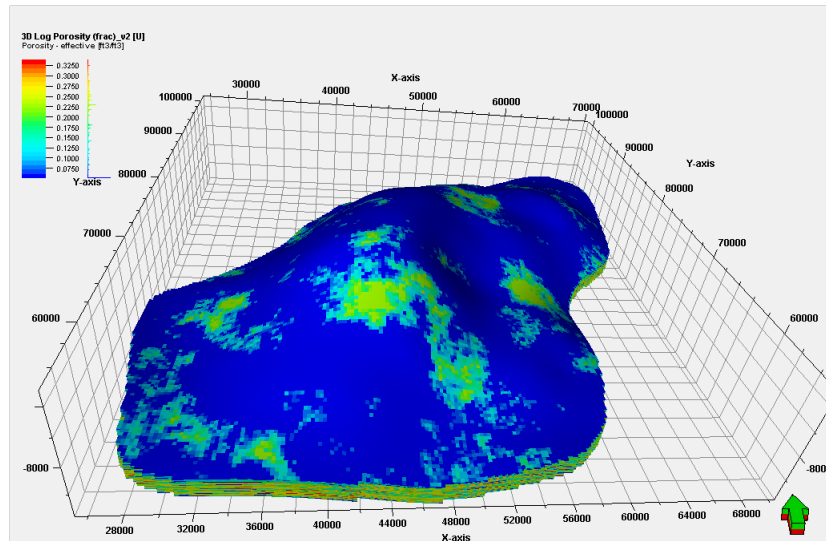


Figure 3.2: COSTA sector model

3.4. Sector Model

For this study, a small sector of COSTA model with 1000 m x 750 m area with an existing vertical well is initially chosen to perform numerical study for CO₂ EOR with huff'n'puff approach. Figure 3.3 shows the chosen sector model with well location. Moreover, figure 3.4 shows a histogram of porosity and permeability within this sector model. It is important to mention that the original COSTA model does not account for any permeability differences in vertical and horizontal directions. Therefore, k_v/k_h ratio is set to be 1 for this study based also on a study conducted on Upper Kharaib carbonate reservoir in U.A.E [35].

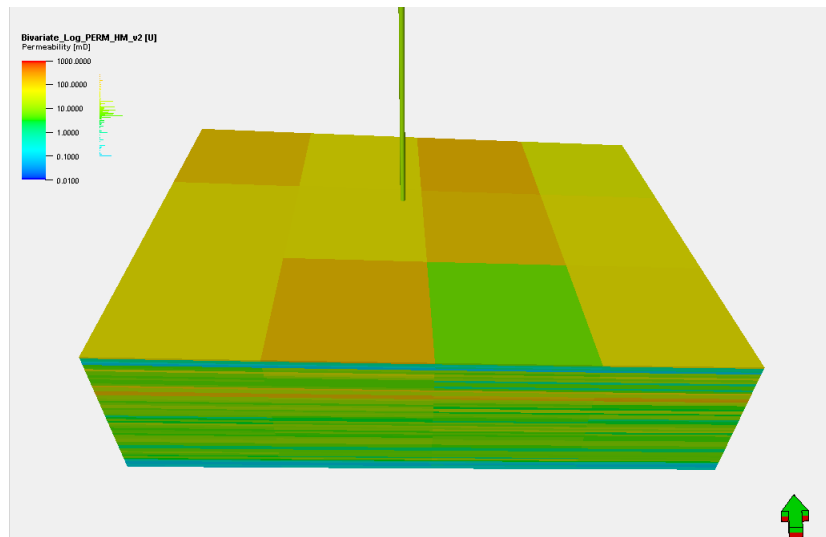


Figure 3.3: Selected sector model for dynamic simulation

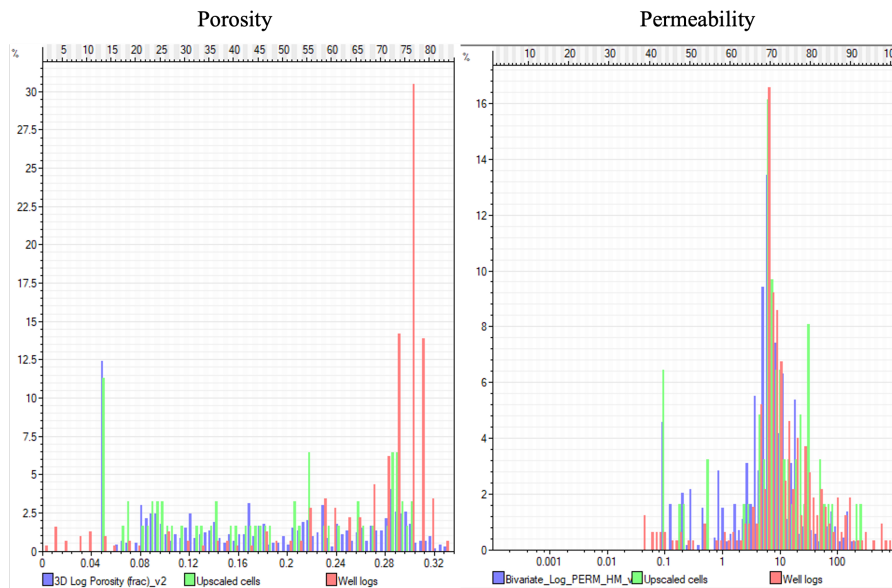


Figure 3.4: Sector model porosity and permeability histogram

3.5. Sector Model Modifications

In order for the sector model to represent an unconventional reservoir, it requires further modifications. The modification is also needed to have a higher model resolution to observe changes during dynamic simulation in the x and y directions.

3.5.1. Permeability Multiplier

A reservoir would be considered unconventional when its permeability is less than 1 mD [36]. Thus, a permeability multiplier of 0.01 K is used for this sector model to represent unconventional reservoir. A 3D permeability distribution of the modified sector model is shown in figure 3.5. In addition, the modified sector model permeability histogram is presented in figure 3.6 highlighting the range of permeability values with a mean value less than 1 mD.

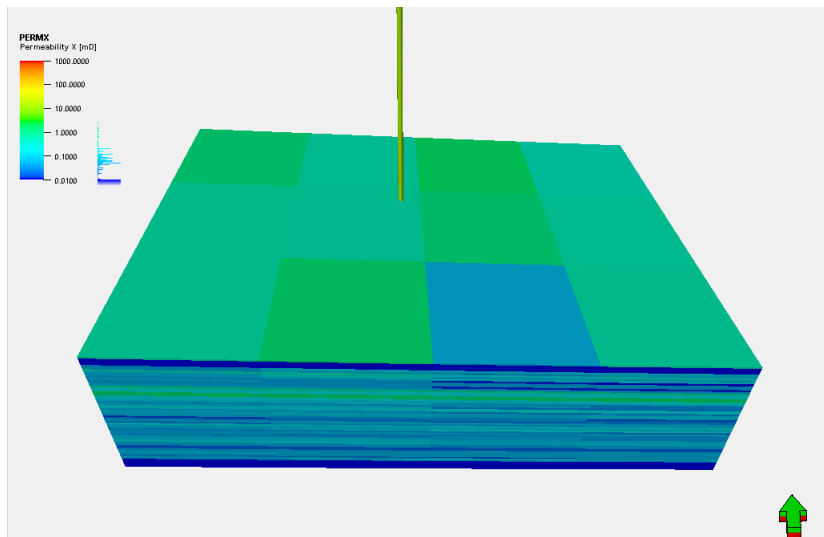


Figure 3.5: Selected sector model after permeability multiplier

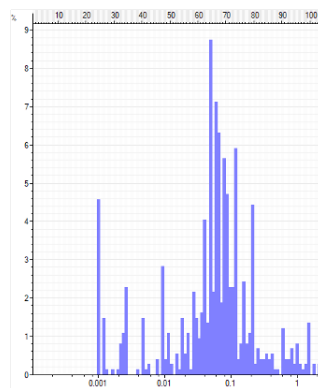


Figure 3.6: Sector model permeability histogram with 0.01 K multiplier

3.5.2. Grid Refinement

In order to improve sector model resolution, each grid cell is split into smaller cells. This would be performed on the areal resolution only since COSTA model captures a high vertical resolution with thickness varying from 0.2 to 2 m. The original areal grid cell size of COSTA model is 250 m x 250 m. Each areal grid cell is split into 100 grid cells with a new grid cell size of 25 m x 25 m in the modified sector model. The modified sector model is shown in figure 3.7 including grid refinement and further cropping of the sector model with a final size of 750 m x 750 m. As can be observed for the figure, the new split cells would still maintain the same petrophysical properties as the original cell. This modified sector model will be used as the static model for reservoir simulation study. The chosen static model size and resolution is based on computational time optimization along with its ability to capture changes in the dynamic simulation. Table 3.1 shows a comparison between three tested model resolutions in terms of grid size and computational time for a base case, where second model resolution is chosen for this study.

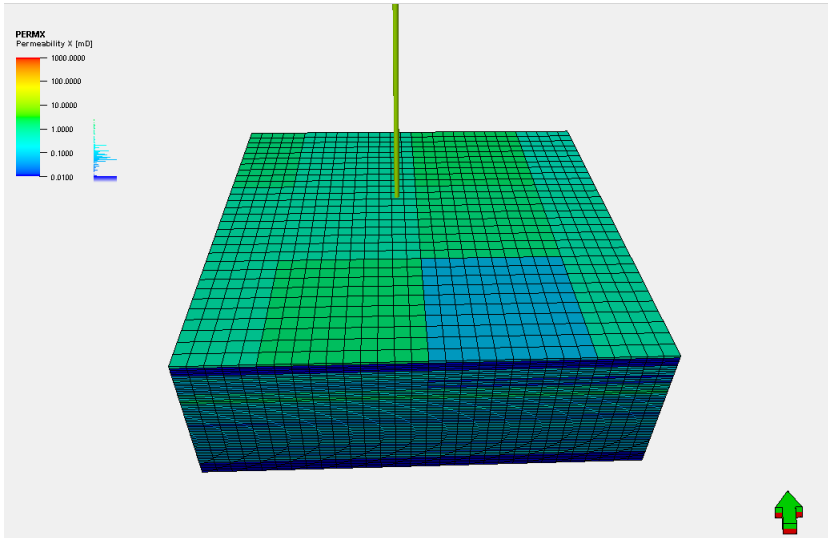


Figure 3.7: Selected sector model after grid refinement

Table 3.1: Model parameters for optimum case

Model Resolution	Grid Size	Model Dimension	Grid Cells	Base Case Run Time (hrs)
1	50 m x 50 m x (0.2 to 2 m)	15 x 16 x 62	14,880	0.23
2	25 m x 25 m x (0.2 to 2 m)	30 x 30 x 62	55,800	4.04
3	50 m x 50 m x (0.2 to 2 m)	60 x 60 x 62	223,200	12

Reservoir Simulation

4.1. Sector Model

Reservoir simulation in this study is performed using Schlumberger ECLIPSE reservoir simulation software E300 [37] along with Schlumberger Petrel software [38] for visualization of results. To simulate reservoir fluids behaviour, compositional run is used with Peng-Robinson Equation of state (EOS). The used sector model for dynamic simulation is 750 m x 750 m x 50 m in size. A total of 55,800 grid blocks are included in the sector model with a 30 x 30 x 62 model dimensions. Each grid cell has a size of 25 m x 25 m with varying thickness from 0.24 to 2.4 m. Simulation of CO₂ injection is computationally demanding and requires optimization on number of grid blocks used in the sector model run. A comparison with other CO₂ EOR numerical studies performed on tight reservoirs are listed in table 4.1 showing that this study uses the highest number of grid cells to simulate CO₂ flooding in a huff'n'puff scheme.

Table 4.1: Model size comparison with literature

Source	Model Size	Grid Size	Model Dimension	Grid Cells
CO ₂ injection for enhanced oil recovery in Bakken tight oil reservoirs [12]	104 m x 396 m x 12 m	6 m x 6 m x 12 m	17 x 65 x 1	1,105
Simulation study of factors affecting CO ₂ Huff-n-Puff process in tight oil reservoirs [39]	1609 m x 1207 m x 15 m	12 m x 12 m x 15 m	132 x 99 x 1	13,068
CO ₂ Utilization for Enhance Oil Recovery with Huff-N-Puff Process in Depleting Heterogeneous Reservoir [40]	381 m x 381 m x 9 m	15 m x 15 m x 2 m	25 x 25 x 6	3,750
Numerical Simulation and Optimization of Enhanced Oil Recovery by the In Situ Generated CO ₂ Huff-n-Puff Process with Compound Surfactant [41]	-	-	29 x 24 x 21	14,616
Reservoir Simulation Study and Optimizations of CO ₂ Huff-n-Puff Mechanisms in Three Forks Formation [23]	762 m x 2134 m x 41 m	13 m x 71 m x 4 m	60 x 30 x 11	19,800
Numerical Simulation and Performance Evaluation of CO ₂ Huff-n-Puff Processes in Unconventional Oil Reservoirs [42]	2000 m x 500 m x 15 m	10 m x 10 m x 5 m	200 x 50 x 3	30,000
Optimization of CO ₂ huff-n-puff EOR in the Bakken Formation using numerical simulation and response surface methodology [43]	572 m x 1829 m x 51 m	-	31 x 30 x 5	11,650
MSc Thesis Model	750 m x 750 m x 50 m	25 m x 25m x (0.2 to 2 m)	30 x 30 x 62	55,800

4.2. Dynamic Reservoir Properties

4.2.1. Reservoir Conditions

In this section, reservoir parameters are based on data from open-source COSTA model [34]. The carbonate reservoir has an anticline structure bearing oil with 42 API and a bottom water aquifer support. The original free water level (FWL) is at a depth of 2478 m. The chosen sector model is located at a depth of 2386 m with a thickness of around 50 m. It is located at the crestal part of the anticline structure above FWL. Thus, the sector model is saturated with reservoir hydrocarbons. Nevertheless, water is present in the formation in the form of connate water based on synthetic MICP provided in COSTA model that will be discussed in relative permeability section. At a datum depth of 2240 m, the reservoir has an initial pressure of 303 bar and an initial temperature of 395 K. The reservoir pressure is above the bubble point pressure of 149.3 bar, which means that it is at an undersaturated state with no free gas. The formation rock has a compressibility of 1.45×10^{-5} 1/bar.

4.2.2. Relative Permeability

Starting with water-oil system relative permeability, it is based on synthetic MICP provided in COSTA model. Since the chosen sector model is located in the oil zone, water-oil system relative permeability is needed to identify connate water saturation (S_{wc}) and residual oil saturation (S_{or}). Different water-oil relative permeability curves for different reservoir rock types (RRTs) were used and normalized to get a representative S_{wc} of 0.38 and S_{or} of 0.13. This would lead to a total immobile fluid ratio of 0.51 in the reservoir. After that, gas-oil system relative permeability is estimated to describe oil displacement during CO_2 injection. Unlike water-oil system relative permeability, there are no MICP data to be used to plot relative permeability curves. Therefore, Corey's method is firstly used to get endpoint relative permeabilities [44]. Residual gas saturation (S_{gc}) and $S_g=1-S_{org}-S_{wc}$ will be used for endpoint gas relative permeability (k_{rg}) calculation. As per a study conducted by [45] to understand CO_2 -oil relative permeability under miscible flooding condition, residual gas saturation would become zero after flooding with the presence of connate water saturation. Therefore, S_{gc} is set to be 0 and maximum S_g is 0.49. To calculate endpoint gas relative permeability, the following equations are used:

$$S_g^* = \frac{S_g}{1 - S_{wc}} \quad (4.1)$$

$$k_{rg} = (S_g^*)^3(2 - S_g^*) \quad (4.2)$$

This results in k_{rg} of 1 at S_{gc} and k_{rg} of 0.607 at $S_g=1-S_{org}-S_{wc}$. The resulting endpoint relative permeabilities are then used to plot gas relative permeability curve for all gas saturation values in between using modified Corey method [45]:

$$k_{rg} = a_g \left(\frac{S_g - S_{gc}}{1 - S_{or} - S_{wc} - S_{gc}} \right)^{b_g} \quad (4.3)$$

Where a_g is the is gas endpoint relative permeability at $S_g=1-S_{org}-S_{wc}$, and b_g is an exponential factor with empirical value of 3.5. The resulting gas relative permeability curve (k_{rg}) is shown in figure 4.1.

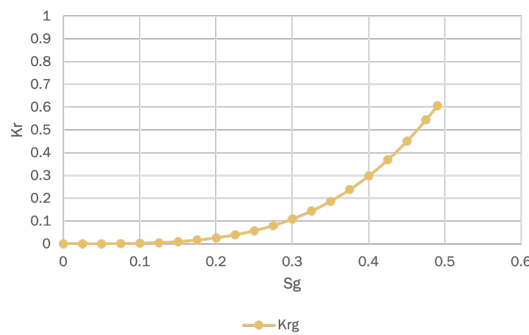


Figure 4.1: Gas relative permeability curve versus gas saturation

As for oil relative permeability curve (k_{rog}) in gas-oil system, it is calculated as a function of S_o using Honarpour method for limestone [46]:

$$k_{rog} = 0.93752 \left[\frac{S_o}{1 - S_{wc}} \right]^4 \left[\frac{S_o - S_{or}}{1 - S_{wc} - S_{or}} \right]^2 \quad (4.4)$$

The resulting oil relative permeability curve as a function of oil saturation is shown in figure 4.2. It starts with an oil saturation from $S_o=S_{or}$ to $S_o=1-S_{wc}$ reaching to a maximum k_{rog} of 0.94. The presented gas and oil relative permeability curves will be used as an input for CO_2 EOR dynamic simulation.

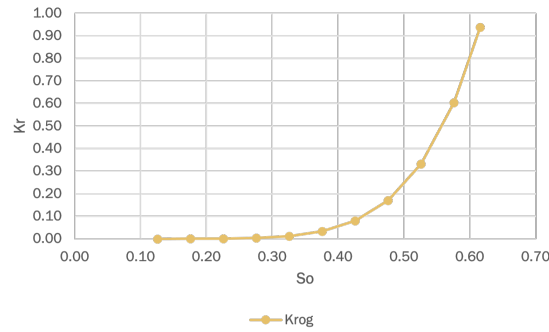


Figure 4.2: Oil relative permeability curve versus oil saturation

4.2.3. Capillary Pressure

To represent capillary forces during gas injection for oil displacement in gas-oil system, capillary pressure curve as a function of gas saturation is calculated using modified Corey method [44]:

$$p_{cgo} = (p_c)_{S_{lc}} \left[\frac{S_g - S_{gc}}{1 - S_{lc} - S_{gc}} \right]^{n_{pg}} \quad (4.5)$$

Where $S_{lc} = S_{wc} + S_{or}$, $(p_c)_{S_{lc}}$ is the capillary pressure at critical liquid saturation and n_{pg} is an exponential factor. $(p_c)_{S_{lc}}$ of 0.5 bars and n_{pg} of 1.5 are used based on lab experiment conducted on a tight rock with similar critical liquid saturation [47]. Figure 4.3 illustrates the resulting capillary pressure curve as a function of gas saturation. Capillary pressure curve is used as an input parameter for CO₂ EOR dynamic simulation.

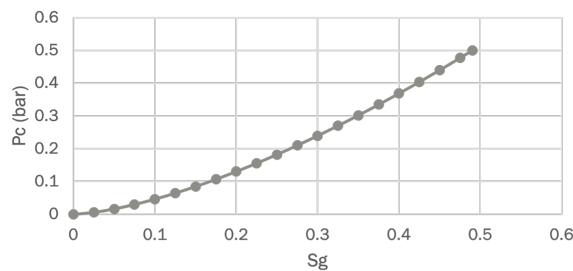


Figure 4.3: Capillary pressure versus gas saturation

4.2.4. Reservoir Fluid Properties

Reservoir and injected fluids characterization is a key aspect in any reservoir simulation study. Since majority of the used geological and dynamic reservoir data are based on COSTA model, it would be preferred to proceed with COSTA model reservoir fluid characterization. Unfortunately, COSTA model uses black oil run that does not include any reservoir fluid composition and does not account for interaction between different components during CO₂ injection. Instead, compositional run is needed to capture the dynamic changes during CO₂ EOR simulation. Therefore, an analogue with similar oil gravity of 42 API as COSTA model is used for fluid characterization. The used analogue is from Bakken oil formation that is a tight formation with similar oil gravity where different studies took place on CO₂ EOR [12]. Table 4.2 includes 7 pseudo components in reservoir oil with its composition, critical properties, molecular weight, acentric factor and parachor values. Moreover, binary interaction coefficients for oil components listed in table 4.3 is used from the same Bakken formation study [12]. Lastly, 0.00864 m²/d CO₂ diffusion coefficient is included as part of the dynamic simulation input parameters since molecular diffusion is a key mechanism in huff'n'puff CO₂ injection in tight reservoirs.

Table 4.2: Reservoir crude oil compositional data for the Peng–Robinson EOS [12]

Component	Mole (%)	Pc (bar)	Tc (K)	Vcrit (m ³ /kg)	MW (g/gmol)	w	Parachor
CO ₂	0.0002	73.8	304.2	0.0021	44.01	0.225	78
N ₂	0.0004	33.9	126.2	0.0032	28.01	0.04	41
CH ₄	0.25	46.0	190.6	0.0062	16.04	0.008	77
C ₂ -C ₄	0.22	43.1	363.3	0.0046	42.82	0.1432	145.2
C ₅ -C ₇	0.2	34.2	511.56	0.0040	83.74	0.2474	250
C ₈ -C ₉	0.13	31.3	579.34	0.0038	105.91	0.2861	306
C ₁₀₊	0.1994	21.9	788.74	0.0046	200	0.6869	686.3

Table 4.3: Binary interaction parameters for oil components [12]

Component	CO ₂	N ₂	CH ₄	C ₂ -C ₄	C ₅ -C ₇	C ₈ -C ₉	C ₁₀₊
CO ₂							
N ₂	-0.02						
CH ₄	0.103	0.031					
C ₂ -C ₄	0.1327	0.0784	0.0078				
C ₅ -C ₇	0.1413	0.1113	0.0242	0.0046			
C ₈ -C ₉	0.15	0.12	0.0324	0.0087	0.0006		
C ₁₀₊	0.15	0.12	0.0779	0.0384	0.0169	0.0111	

Assessment of CO₂ EOR Performance

In this chapter, a comprehensive evaluation of CO₂ EOR performance in tight oil reservoir with a huff'n'puff scheme will be presented and discussed utilizing numerical simulation. Initially, a base case scenario will be used as a starting point, where the need of primary recovery period will be assessed in order to set an optimum starting time for CO₂ EOR. A discussion on the ongoing physical mechanisms that take place at each stage during the CO₂ EOR process will follow. Then, a detailed sensitivity study will be presented and discussed including many parameters that can have an influence on CO₂ EOR performance and resulting oil recovery. Lastly, an optimum case will be presented based on the findings from the sensitivity study. The optimum case objective is to generate the highest oil recovery within a projected lifetime of 20 years.

5.1. Base Case

In order to initiate the evaluation of CO₂ EOR performance, a scenario is chosen as a base case. The parameters used for this base case are presented in table 5.1. All rates that are presented and discussed are at surface conditions. In this base case, CO₂ EOR will commence from the original reservoir conditions with no primary recovery period. The simulation results of base case are illustrated in figure 5.1. Results of oil production rate and cumulative oil production show that oil recovery is higher at earlier periods of CO₂ EOR and relatively declines with time. This is because of the challenge to produce oil in further areas from the well location in this tight reservoir at later times. As for gas production, it accounts for both injected CO₂ reproduction and solution gas. Eventhough CO₂ injection is introduced, reservoir pressure experiences a decline with time due to the production of both oil and injected CO₂.

Table 5.1: Model input parameters for base case

Parameter	Value
Lifetime, years	20
Production bottomhole pressure constraint, bars	100
Injection rate, mm ³ /d	0.025
Injection time per cycle, days	60
Soaking time per cycle, days	30
Production time per cycle, days	60
Number of cycles	49

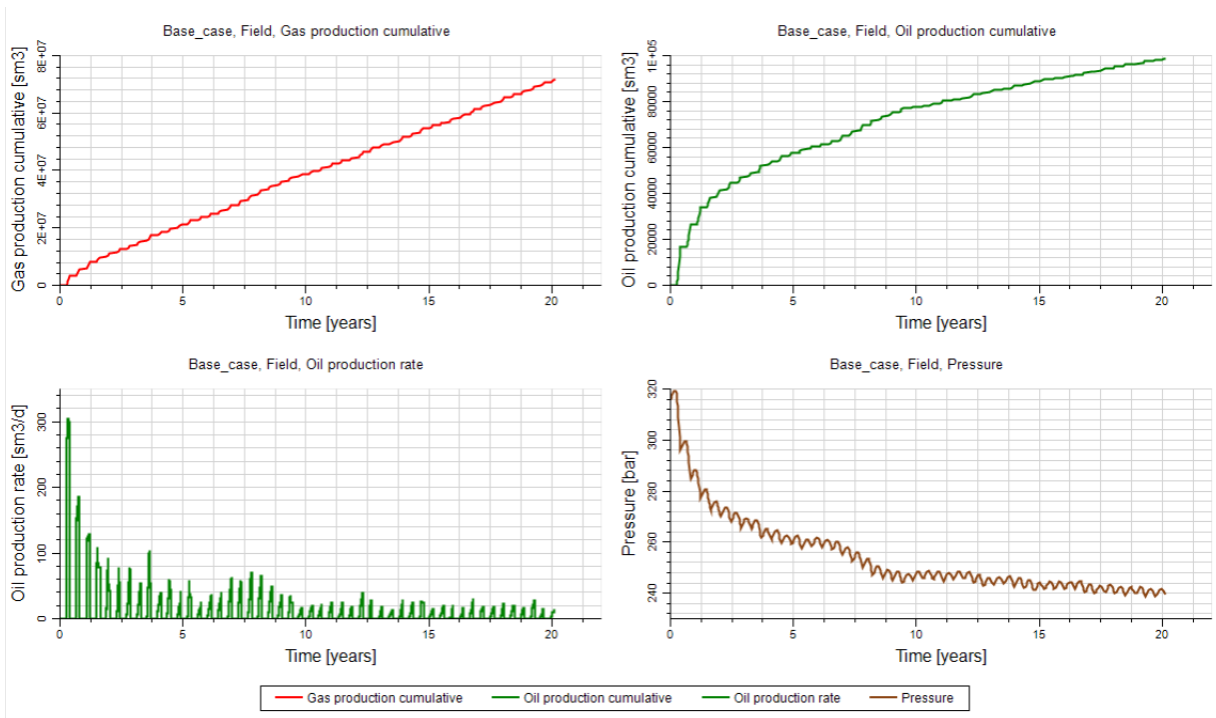


Figure 5.1: Simulation Results of base case

5.1.1. Primary Recovery

In order to assess the added value of EOR in terms of oil recovery, it has to be compared to natural depletion case. In figure 5.2, cumulative oil production of both cases are shown highlighting additional gain from CO₂ EOR at the end of lifetime. However, it can be observed that natural depletion case results in much higher oil recovery at the first two years of the simulation compared to the base case, and then starts to plateau with no oil production for the remaining years. This indicates that at the first two years, the reservoir has the ability to produce naturally at the bottomhole pressure constraint with more oil gain than the base case. This is attributed to the initial reservoir pressure that can maintain oil production for the first two years with no pressure support. Including CO₂ EOR results in injection and shut-in periods that would reduce cumulative oil production. In addition, production of injected CO₂ back would hinder oil production due to the effect of slippage [4].

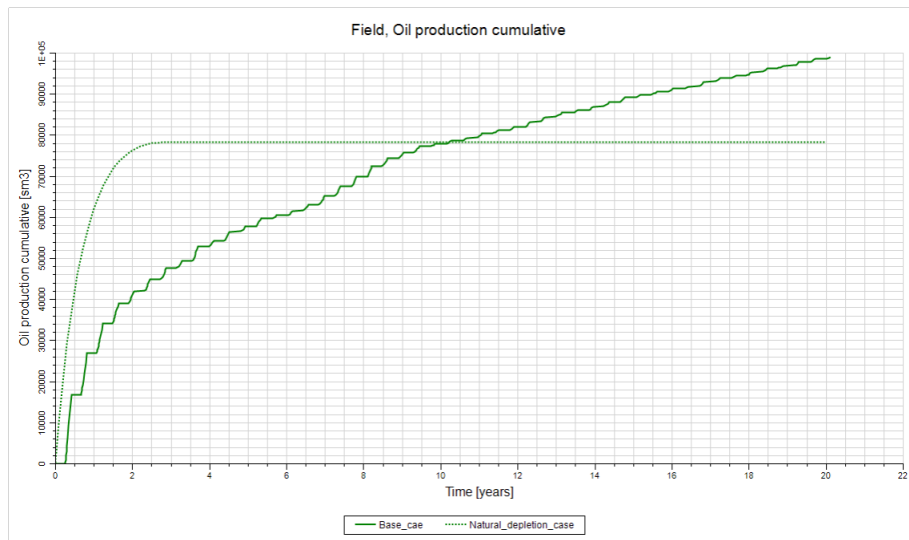


Figure 5.2: Cumulative oil production of base case and natural depletion case

A new case is tested to shift the starting time for CO₂ EOR by introducing a primary recovery period at the first 600 days. This would reduce the number of cycles in the new case from 49 to 45 cycles. The resulting cumulative oil production in figure 5.3 shows that introducing a primary recovery period prior to CO₂ EOR would yield the highest oil recovery. Therefore, this will become the new base case and it will be called the modified base case.

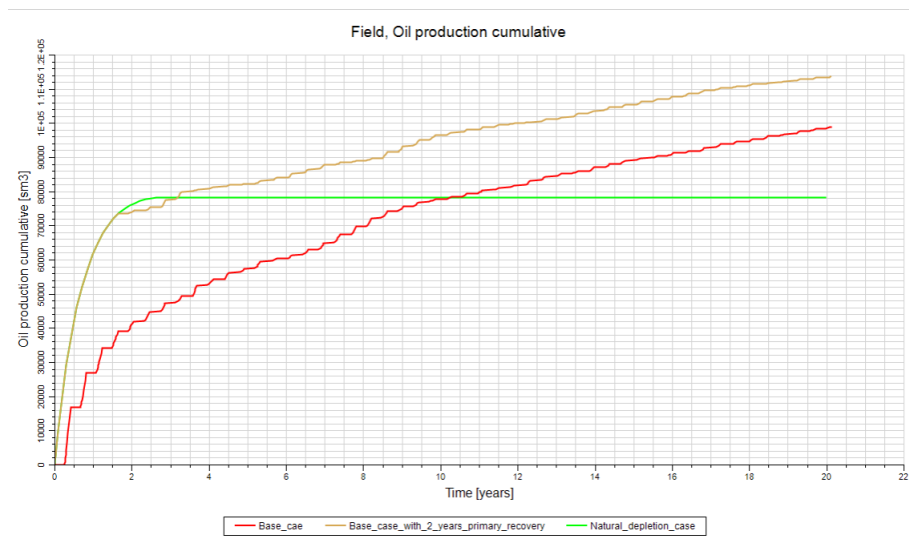


Figure 5.3: Cumulative oil production with primary recovery period

As observed, it is highly important to evaluate and assess the optimum starting time for CO₂ EOR to obtain highest oil recovery. Including a primary recovery period in the reservoir development plan would not only result in higher oil recovery, but also lower CO₂ utilization by reducing the number of cycles. The time can vary depending on reservoir conditions and bottomhole pressure constraints. It can also be influenced by the pressure drawdown generated by low permeability in targeted zones depending on reservoir heterogeneity and well contact area.

5.1.2. Injection Stage

After including primary recovery period before CO₂ EOR, the reservoir will experience a pressure decline as shown in figure 5.4 due to oil withdrawal. Once the first injection cycle of CO₂ is performed, a pressure build up occurs. It is observed that the highest pressure build up is located near the well location. This is due to the low reservoir permeability that limits the flow of CO₂ and pressure propagation into the entire sector model in order to achieve equilibrium. CO₂ transports in the oil reservoir via two different flow mechanisms: mechanical dispersion and molecular diffusion. The difference between the two mechanisms is that CO₂ will spread into the reservoir due to pressure gradient in mechanical dispersion mechanism, while in molecular diffusion it will spread due to concentration gradient. Since this is a tight reservoir, mechanical diffusion would be the dominant transport mechanism. [19] divided CO₂ huff'n'puff transport into flow sweep and diffusion sweep. Flow sweep refers to CO₂ movement under the influence of pressure difference, and diffusion sweep refers to the CO₂ movement under the influence of diffusion.

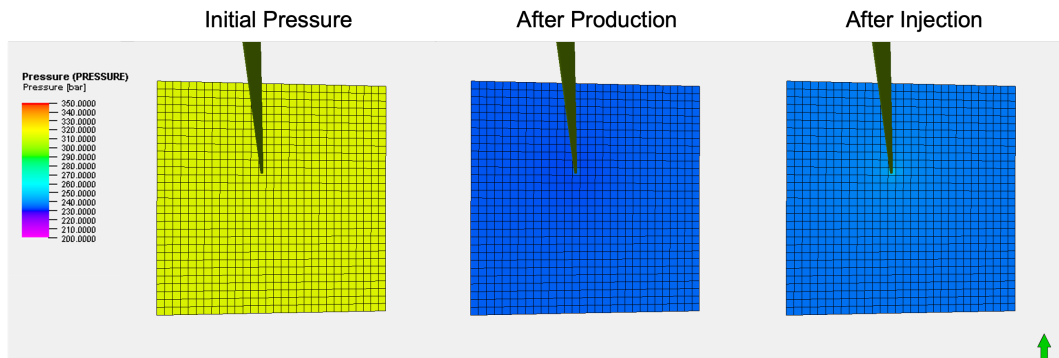


Figure 5.4: Pressure map from initial time until first injection cycle

Once CO₂ comes into contact with the reservoir oil, it will dissolve in it. With time, a reduction in interfacial tension between CO₂ and oil will occur since the injection is under miscible conditions. The influence of those two EOR mechanisms will be discussed in Production Stage section. Figure 5.5 highlights the injected gas saturation distribution in the reservoir model post first injection cycle. It can be observed that injected gas saturation is concentrated around the well, especially in the upper layers. Additional cross-section plot of reservoir permeability is shown on the same figure to correlate gas saturation distribution with reservoir permeability. The reasons behind having higher gas saturation in the upper layers are reservoir heterogeneity and buoyancy forces. Upper reservoir layers have higher permeability values resulting in easier injection pathways and higher gas saturation. Buoyancy forces are also acting on injected CO₂ at its supercritical state due to the difference in densities with reservoir oil leading to CO₂ upward movement and accumulation in the upper interval.

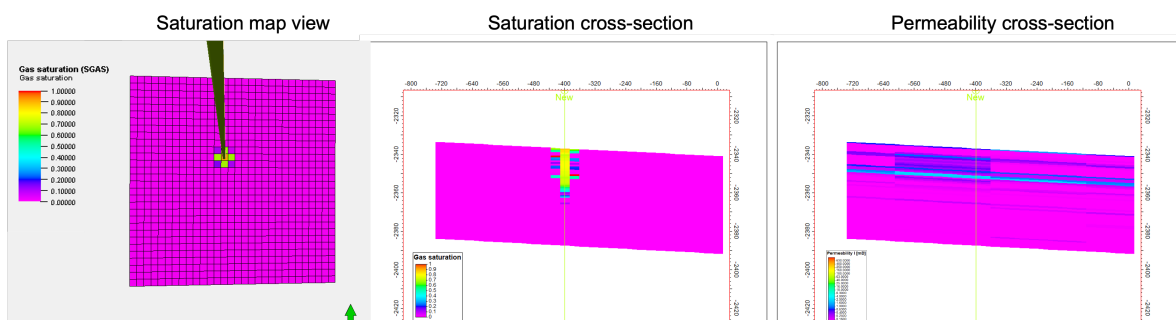


Figure 5.5: Gas saturation map after first injection period

5.1.3. Soaking Stage

In the huff'n'puff scheme, each injection cycle is followed by a soaking period. The objective of the soaking period is to allow for more time for CO₂ to transport deeper into the formation mainly through molecular diffusion. This would be dependent on CO₂ diffusivity that will be discussed in the sensitivity study section. The additional time for CO₂ transport would allow it to come into contact with larger volume of reservoir oil, leading to more CO₂ dissolution and higher oil recovery during production. This would be tested and discussed in soaking time sensitivity study section. The changes in injected gas saturation shown in figure 5.6 illustrates CO₂ transport after soaking period. The high gas saturation areas before soaking are distributed to new areas after soaking. This means that diffusion is taking place during soaking, where gas is moving due to CO₂ concentration gradient.

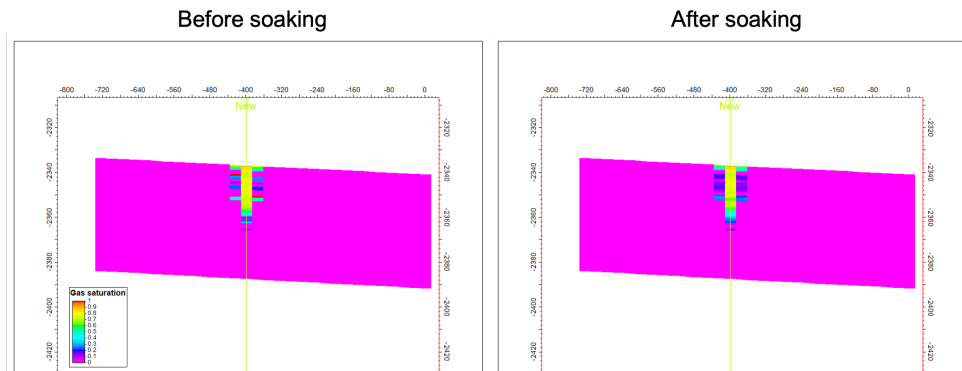


Figure 5.6: Gas saturation map after first soaking period

In terms of pressure changes, the reservoir pressure doesn't experience noticeable changes during soaking periods as shown in figure 5.7. However, the pressure is distributed during soaking period in order to achieve pressure equilibrium within the reservoir as can be seen in figure 5.8.

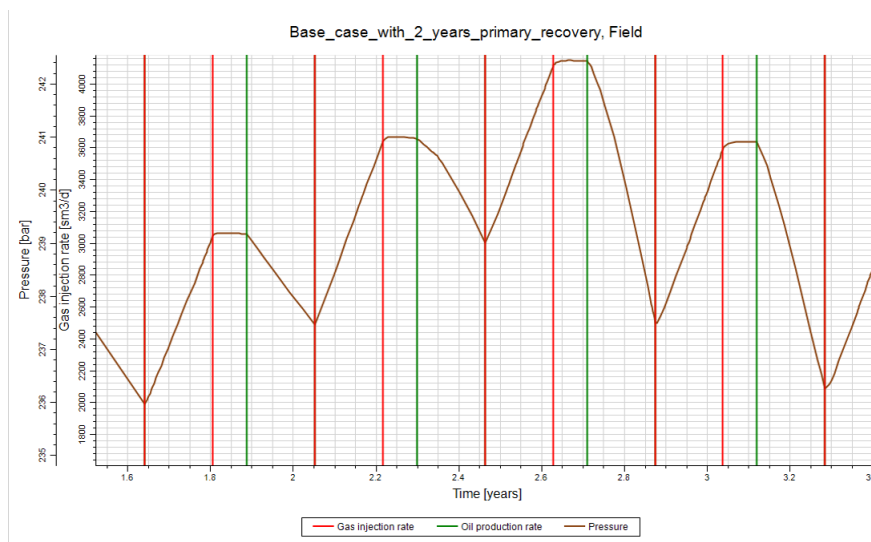


Figure 5.7: Pressure profile in huff'n'puff cycles

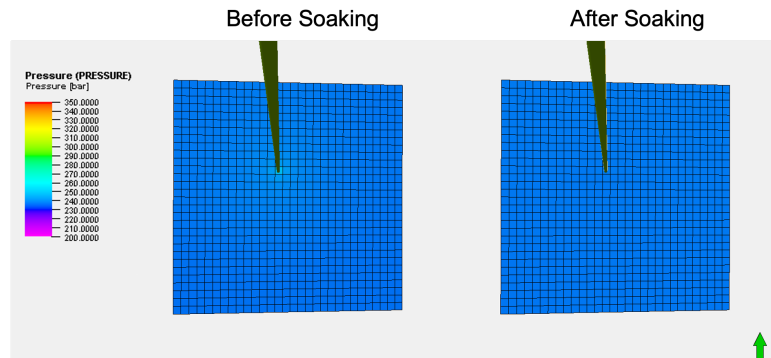


Figure 5.8: Pressure map before and after soaking

5.1.4. Production Stage

The last stage of each huff'n'puff cycle is production. During production stage, both oil and CO₂ would be produced. The production in CO₂ EOR relies on many advantages over natural production in primary recovery. One advantage is the reservoir pressure buildup generated during CO₂ injection in each cycle. Dissolved CO₂ in oil during injection and soaking is able to generate effect of dissolved gas drive [16]. This drive would allow for higher oil recovery compared to natural production since it offers higher pressure gradient between reservoir and bottomhole pressure during production. Another advantage is the improved oil mobility after CO₂ dissolution. The dissolved CO₂ in oil will result in swelling of reservoir oil and reduction in its viscosity leading to an improvement in mobility during production resulting in higher oil recovery.

The amount of CO₂ dissolution is dependent on two controlled parameters: dissolution rate and time. Injection pressure has an influence on dissolution rate, as higher injection pressures would lead to higher dissolution rate of CO₂ in oil [11]. As for dissolution time, it is controlled by the injection and soaking durations. The influence of time on dissolution will be verified and discussed in the sensitivity study section. From the modified base case simulation results, the amount of CO₂ dissolution can be inferred from GOR plot in figure 5.9. The GOR spikes at the beginning of each production cycle indicate that not all injected CO₂ had dissolved. In fact, some of the injected CO₂ is reproduced in the form of free gas. Based on that, the production period can be divided into two main parts: free gas production with some oil, and oil with dissolved gas production. The free and dissolved gas production can also be observed by the changes in gas saturation after the first production cycle in figure 5.10. Having higher dissolution would reduce the amount of free gas around the well and enhance oil production. Therefore, CO₂ dissolution plays a major role in not only oil recovery, but also CO₂ utilization.

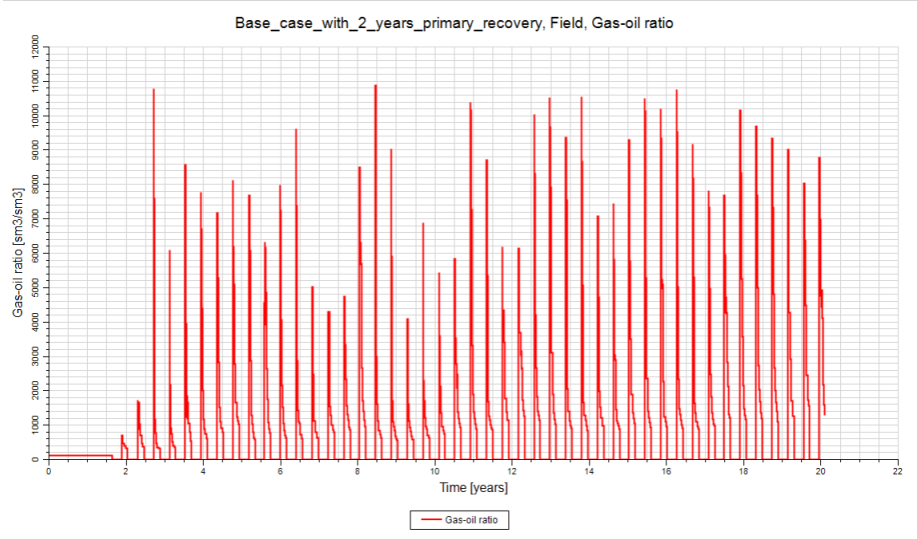


Figure 5.9: Production gas-oil ratio plot

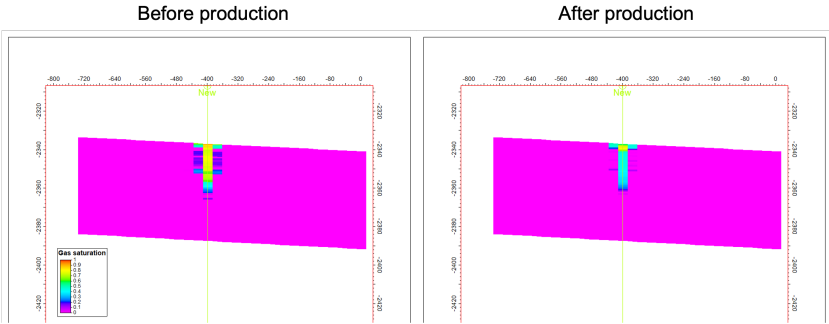


Figure 5.10: Gas saturation map after first EOR production period

In the huff'n'puff scheme, not all injected CO₂ is reproduced. In fact, a significant volume of injected CO₂ is stored in the reservoir. Figure 5.11 highlights the difference between cumulative gas injection and production, showing a higher cumulative gas injection during the 20 years lifetime. This is with the inclusion of solution gas production with CO₂ as a total gas production.

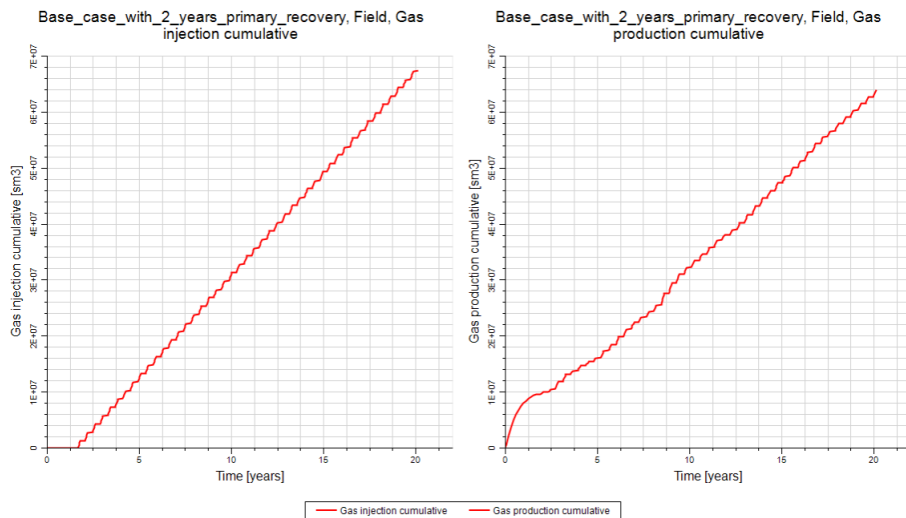


Figure 5.11: Cumulative gas injection and production

5.2. Sensitivity Study

In this section, a detailed evaluation of the impact of different parameters on the cumulative oil production is presented and discussed. It also includes a description of main mechanisms leading to the resulting impact. The strategy is to build an optimum CO₂ EOR huff'n'puff case based on the findings from each sensitivity parameter and include it in the next case. Each part would end with a comparison with any previous studies done in terms of numerical simulation. The starting case would be the modified base case that includes primary recovery period.

5.2.1. Injection Rate

To evaluate injection rate, the same input parameters presented in table 5.1 are used, with the reduction of number of cycles to 45 due to the addition of a primary recovery period at the beginning. Six different injection rates are tested: 0 mm³/d, 0.01 mm³/d, 0.025 mm³/d, 0.05 mm³/d, 0.075 mm³/d, 0.1 mm³/d. Cumulative oil production results in figure 5.12 show that an injection rate of 0.025 mm³/d would yield the highest oil recovery at the end of the lifetime. With a closer look into the cumulative oil production results, figure 5.13 presents the difference in cumulative oil production between different injection rates. Based on the results, an increase in injection rate would lead to a higher cumulative oil production, until an optimum injection rate is reached. At injection rates higher than the optimum rate, the cumulative oil production would decline.

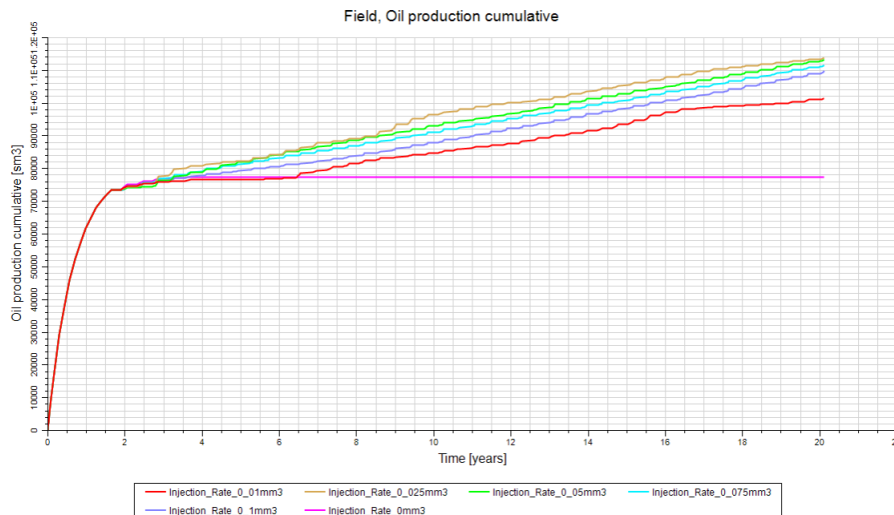


Figure 5.12: Cumulative oil production plots at different injection rates

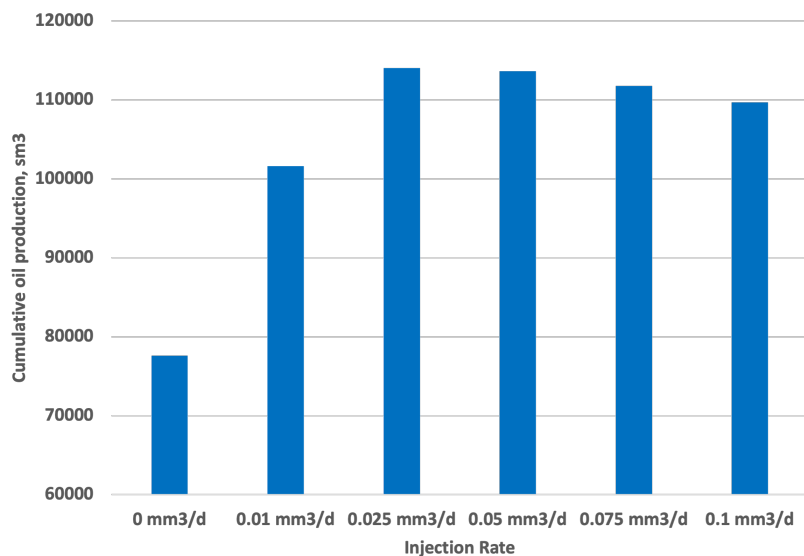


Figure 5.13: Cumulative oil production at different injection rates

To understand the reasons behind the changes in cumulative oil production at different injection rates, one must look at the physical influence of injection rate on CO₂ EOR mechanisms. First, the increase in injection rate would lead to an increase in injection pressure. As discussed earlier, there is a direct relation between injection pressures and dissolution rates. This means that the increase in injection pressure would have a positive influence on dissolution rate, which can lead to higher oil recovery. However, this would add value to a certain limit because of CO₂ transport limitation in tight reservoirs. The high dissolution rate would not be beneficial once CO₂ exposed area in the reservoir is fully saturated. This would lead to an accumulation of free gas around the well in the cases of high injection rates, leading to higher gas production as shown in figure 5.14. The high gas production can hinder oil production as discussed previously. Since the dominant CO₂ transport mechanism is molecular diffusion in tight reservoirs, higher injection pressures would have a minor impact on CO₂ exposure area within the reservoir. Diffusion coefficient and injection and soaking periods are the main factors controlling this exposure area of CO₂ in a given reservoir conditions. This will be verified and discussed in the sensitivity study. Therefore, for a given injection and soaking time, there

would be an optimum injection rate to yield the highest oil recovery.

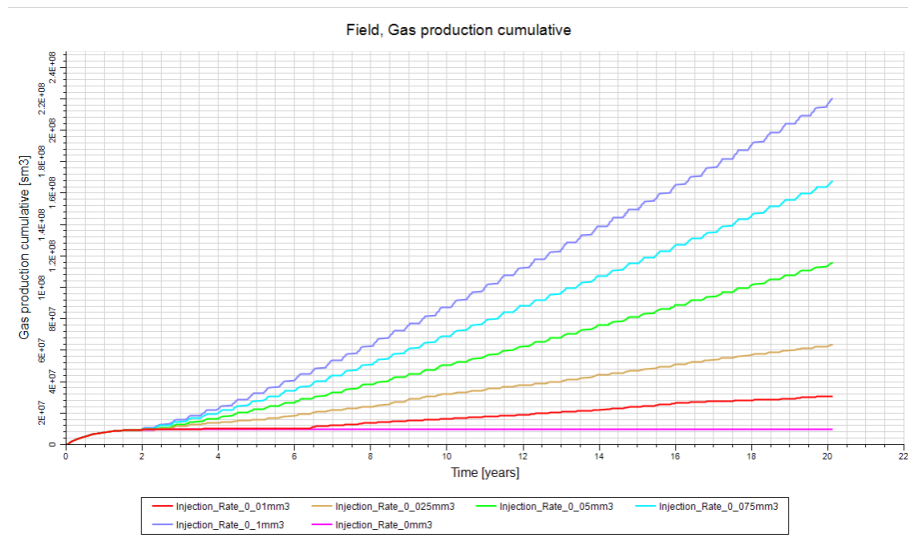


Figure 5.14: Cumulative gas production at different injection rates

Comparing the findings with previous work done in the literature, four different studies were conducted on the influence of injection rates on oil recovery using numerical simulation. Two of those studies reached to a similar conclusion that oil recovery would increase with the increase in injection rate until an optimum injection rate is achieved [48][42]. The third study concluded that once the optimum injection rate is achieved, higher injection rates would not result in any oil gain nor decline [23]. The last study concluded that the injection rate is always directly related to oil recovery [39].

5.2.2. Injection Time

Building on the findings from injection rate sensitivity, injection time is evaluated by testing 7 different injection durations per cycle: 10 days, 30 days, 60 days, 90 days, 120 days, 150 days and 180 days. In this test, production and soaking periods are maintained the same while changing total lifetime period depending on injection time in each scenario. This is to have comparable results and conclusive understanding of the influence of injection time while keeping other parameters constant. The test is performed using the same modified base case parameters while using the optimum injection rate of $0.025 \text{ mm}^3/\text{d}$ based on previous findings. Simulation results of cumulative oil production in figures 5.15 and 5.16 show that the highest oil recovery will be achieved with an injection time of 150 days. Results show that oil recovery increases with longer injection time until an optimum injection time is reached. Cumulative oil production would decline at higher injection times as can be seen in 180 days injection scenario.

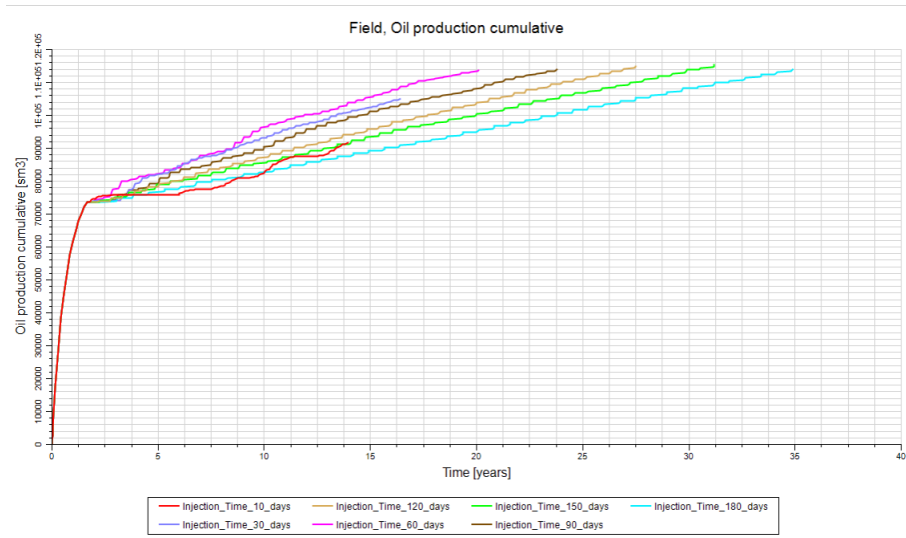


Figure 5.15: Cumulative oil production plots at different injection durations

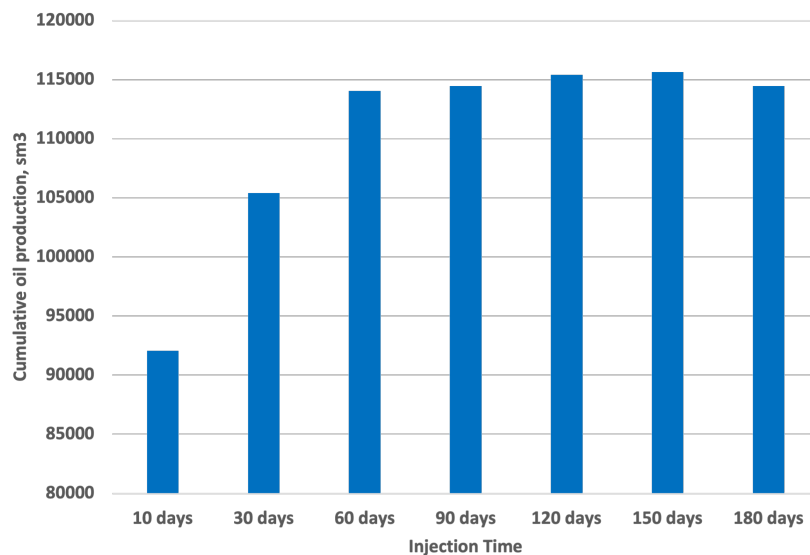


Figure 5.16: Cumulative oil production at different injection durations

The changes in cumulative oil production at different injection times can be explained by several CO₂ EOR mechanisms. One is the reservoir pressure increase due to higher injected CO₂ volume with longer injection duration at the same injection rate. As discussed previously, the increase in pressure will result in higher dissolution rate of CO₂ in oil leading to higher oil recovery during production stage. Similar to the understanding in injection rate sensitivity study, higher CO₂ injected volumes can be beneficial up to a certain optimum value in a given reservoir conditions. Beyond this optimum volume, free gas will hinder oil production leading to a decline in cumulative oil production. Another mechanism that enhances oil recovery with higher injection times is longer CO₂ transport and dissolution time. Figure 5.17 shows gas saturation distribution comparison after first injection cycle between 10 days and 150 days injection time cases. This illustrates the influence of injection time on CO₂ transport contacting larger area of the reservoir leading to higher recovery. Therefore, for a given injection rate, there would be an optimum injection time to yield the highest oil recovery. In this case, 150 days scenario resulted in the highest oil recovery, but with a longer lifetime. To determine the optimum injection time scenario with respect to CO₂

EOR lifetime, figure 5.18 is presented to highlight incremental oil gain per day for the additional project lifetime. It can be concluded that 60 days injection time would be the optimum injection time with respect to oil gain per day. At injection time scenarios higher than 60 days, additional oil gain per day is very low making it economically unfeasible.

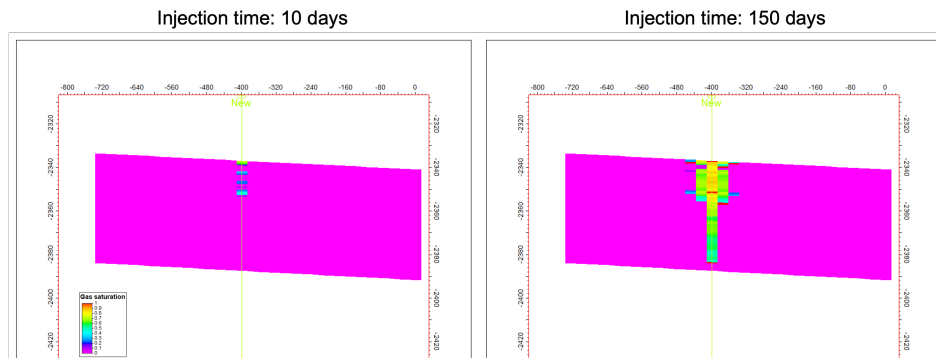


Figure 5.17: Gas saturation cross section map after first injection cycle

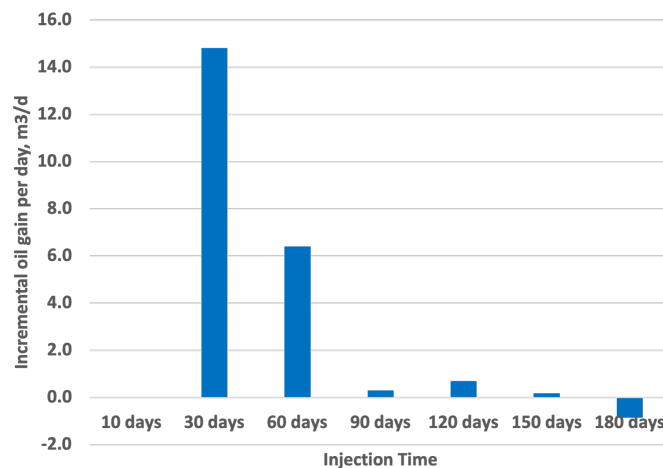


Figure 5.18: Incremental oil gain per day for the additional lifetime needed

Comparing the findings with previous work done in the literature, three different studies were conducted on the influence of injection time on oil recovery using numerical simulation. Two of those studies reached to a similar conclusion that oil recovery would increase with the increase in injection time until an optimum injection time is achieved [48][42]. The third study concluded that the injection time is always directly related to oil recovery since it leads to higher injected volumes [23].

5.2.3. Injection Time at Constant Volume

During the evaluation of injection time on oil recovery, another parameter is changing alongside time which is injection volume. Another approach is followed where injection volume is kept constant by changing injection rate to observe the influence of injection time and confirm previous findings. Four different cases are tested with a fixed injection volume of 3.75 mm^3 per cycle. The cases are shown in table 5.2 with their corresponding injection times and rates. The resulting cumulative oil production for these cases are shown in figures 5.19 and 5.20 with a direct relation between injection time and oil recovery. There is a realized cumulative oil production increase of 7% when comparing first and last case. Thus, higher injection time with fixed injection volume would lead to higher oil recovery.

Table 5.2: Different injection cases at fixed injection volume

Case	Injection Time (days)	Injection Rate (mm ³ /d)
1	37.5	0.1
2	50	0.075
3	150	0.025
4	375	0.01

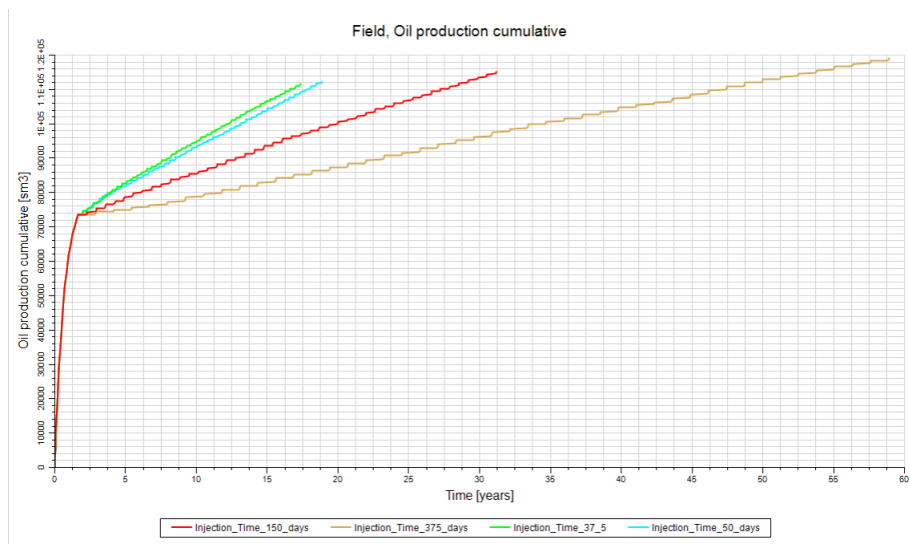


Figure 5.19: Cumulative oil production plots at different injection durations with fixed volume

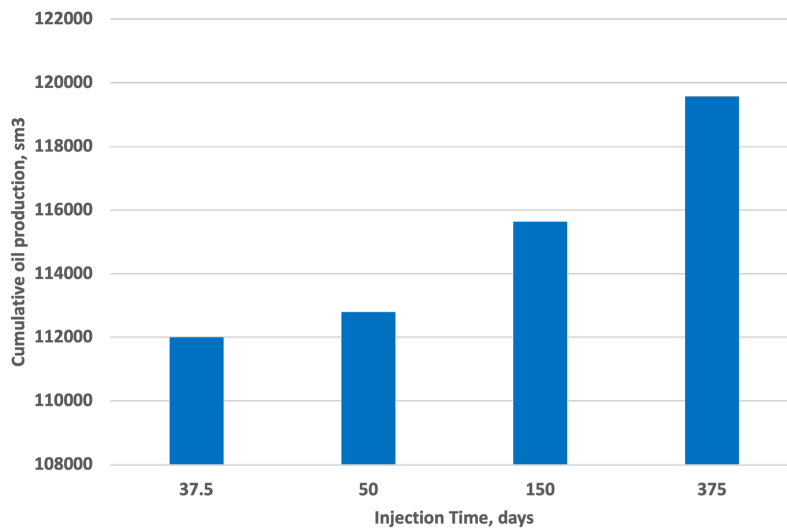


Figure 5.20: Cumulative oil production at different injection durations with fixed volume

The influence of injection time on oil recovery confirms previous findings. Longer injection time allows for more CO₂ transport and dissolution time as indicated by cumulative gas production in figure 5.21. Lower gas production with longer injection time is a result of higher CO₂ dissolution and lower free gas volume to

be reproduced. Although injection rate is reduced at higher injection times, the impact of lower pressure support on dissolution rate is insignificant. This indicates that time factor has a higher influence on oil recovery than injection rate in tight reservoirs. This approach of evaluating injection time using a fixed injected volume on CO₂ EOR has not been covered in previous CO₂ EOR numerical studies on tight oil reservoirs.

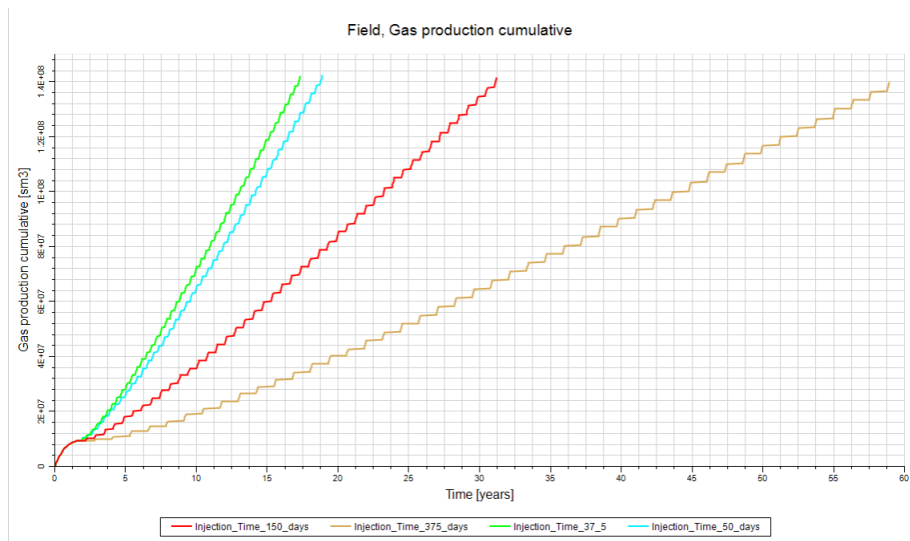


Figure 5.21: Cumulative gas production plots at different injection durations with fixed volume

5.2.4. Soaking Time

One of the key parameters in CO₂ EOR huff'n'puff is soaking time. In this study, soaking time is evaluated using the modified base case including the optimum injection rate and time scenario from previous findings. Six different soaking times are tested: 0 days (without soaking), 7 days, 10 days, 30 days, 90 days and 120 days. Production and injection periods are maintained the same while changing the total lifetime period depending on soaking time in each scenario in order to have comparable results and conclusive understanding on the influence of soaking time while keeping other parameters the same. Cumulative oil production results in figures 5.22 and 5.23 show that the highest oil recovery is achieved with a soaking time of 90 days. Results show that oil recovery increases with longer soaking time until an optimum time is reached. Once soaking time exceeds the optimum value, cumulative oil would decline, as can be seen in 120 days soaking scenario.

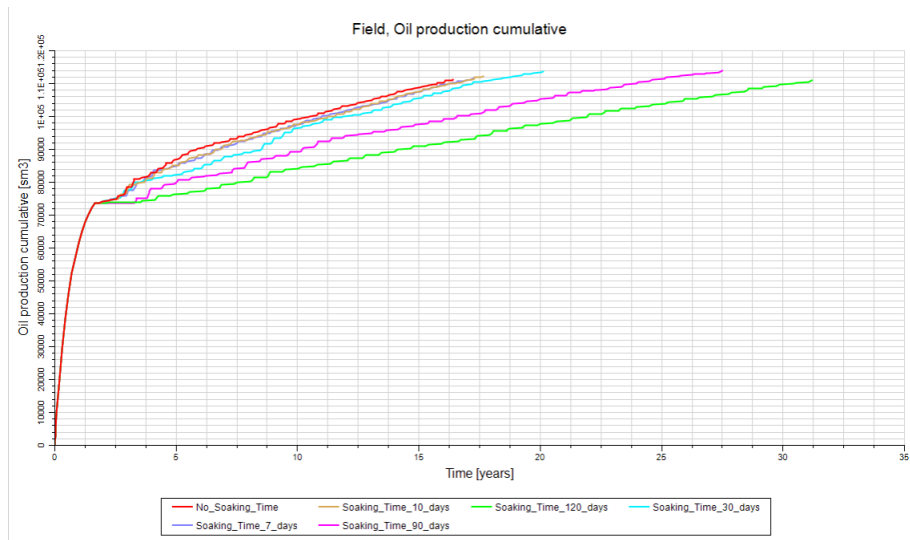


Figure 5.22: Cumulative oil production plots at different soaking periods

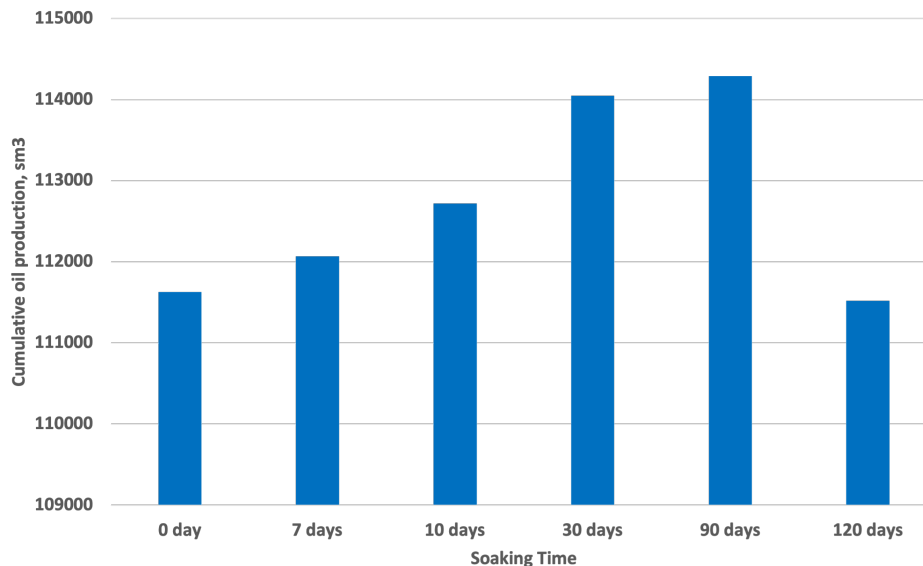


Figure 5.23: Cumulative oil production at different soaking periods

The influence of soaking during CO₂ EOR huff'n'puff has been discussed in the soaking stage section. Cumulative gas production results in figure 5.24 confirm the impact of soaking through diffusion and dissolution as longer soaking time would lead to lower cumulative gas production. Nevertheless, the relation between soaking time and oil recovery is not always proportional. Too long soaking time would lead to a reduction in injected CO₂ concentration around the well that will be insufficient for oil displacement during production stage. This is observed in gas saturation distribution before and after soaking in figure 5.25 for 120 days soaking time case. Even though the highest oil recovery is achieved with 90 days of soaking, the optimum soaking time is to be determined following the incremental oil gain per day for the additional project lifetime approach. Results in figure 5.26 show that 30 days soaking time would be the optimum time with respect to oil gain per day. At longer soaking time, additional oil gain per day is very low making it economically unfeasible. Therefore, a soaking time of 30 days is chosen as the optimum time in this study.

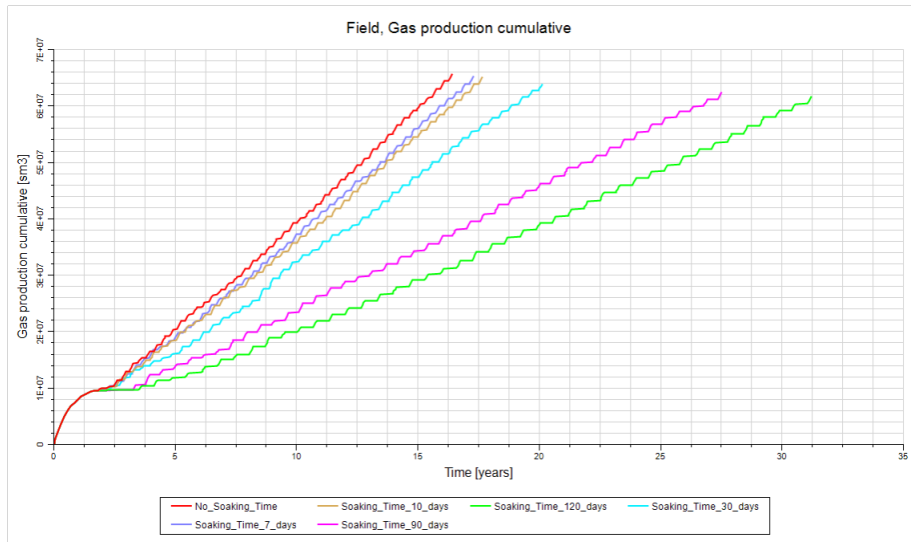


Figure 5.24: Cumulative gas production plots at different soaking periods

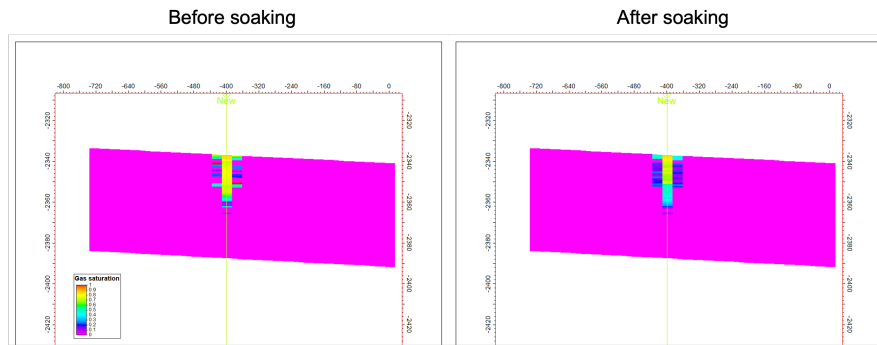


Figure 5.25: Gas saturation cross section map for 120 days soaking time case

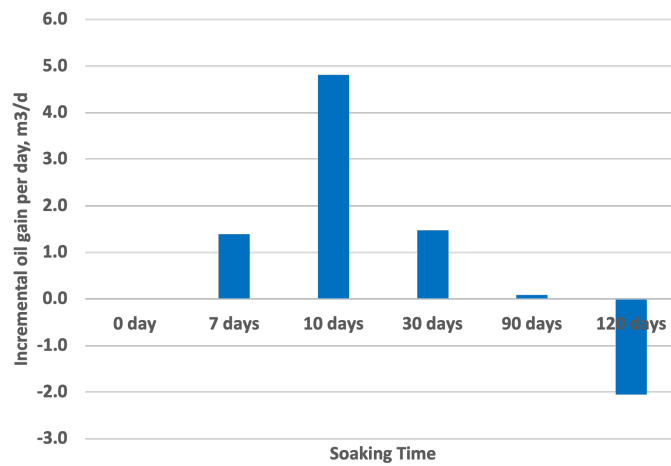


Figure 5.26: Incremental oil gain per day for the additional lifetime needed

Comparing the findings with previous work done in the literature, two different studies were conducted on

the influence of soaking time on oil recovery using numerical simulation. They both reached to a similar conclusion that oil recovery would increase with the increase in soaking time until an optimum time is achieved [48][42]. In both studies, 30 days is chosen as the optimum soaking time in agreement with this study as well.

5.2.5. Production Time and Number of Cycles

Another key parameters to be evaluated are production time and number of cycles. At a fixed project lifetime, number of cycles will be determined based on optimum injection, soaking and production periods for each cycle. In this study, production time and number of cycles are evaluated together at a fixed lifetime using optimum injection and soaking times from previous findings. Six different cases of production time and number of cycles are evaluated as listed in table 5.3 while maintaining a fixed project lifetime of around 20 years. Cumulative oil production results in figures 5.27 and 5.28 show that the highest oil recovery will be achieved with a production time of 150 days and 28 cycles. Results show that oil recovery increases with longer production time and less cycles until an optimum time is reached. At longer production period and less cycles, cumulative oil would decline as can be seen in case 6.

Table 5.3: Production time and number of cycles cases at a fixed project lifetime

Case	Production Time (Days)	Number of Cycles
1	30	56
2	60	45
3	90	37
4	120	32
5	150	28
6	365	15

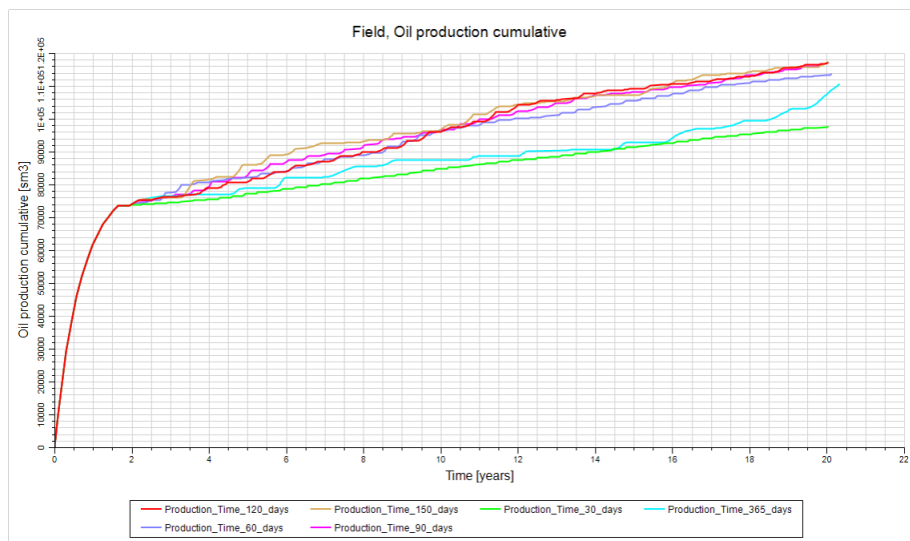


Figure 5.27: Cumulative oil production plots at different production periods

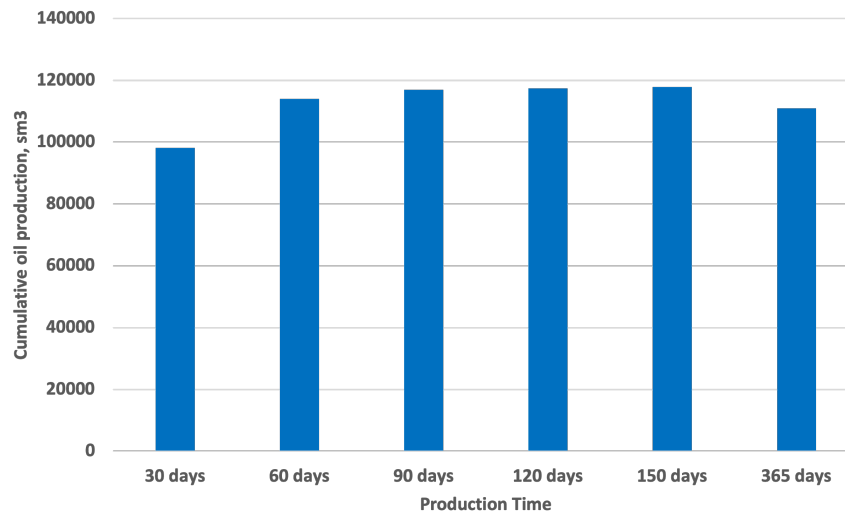


Figure 5.28: Cumulative oil production at different production periods

Results have to be analyzed from both production time and number of cycles aspects. For production time, extending the duration would give the ability to maximize oil recovery after each injection and soaking stage in each cycle. However, the increase in production time is beneficial up to a point where oil is unable to follow due to pressure drop requiring another cycle of injection. Therefore, there would be an optimum production time to achieve maximum oil recovery without non-flow time to be wasted. As for the number of cycles, it controls the amount of CO₂ injected volume and pressure support in a fixed lifetime. Having large number of cycles can lead to large injected CO₂ volume that will accumulate around the well and backflow during production stage hindering oil recovery as explained previously in injection rate and time sensitivity sections. On the other hand, having low number of cycles would lead to low CO₂ injected volume that will limit the swept area for oil recovery. Based on that, there would be an optimum number of cycles at a fixed lifetime to achieve highest oil recovery with an optimized CO₂ utilization. In this study, 150 days of production time with 28 cycles is considered optimum with respect to oil recovery and CO₂ utilization.

Comparing the findings with previous work done in the literature, two different studies were conducted on the influence of number of cycles on oil recovery using numerical simulation. First study concluded that oil recovery increases with more cycles reaching to an optimum of 3 cycles [12]. Similarly, the second study reached to the same conclusion that more cycles will result in higher oil recovery until reaching an optimum of 8 cycles [42]. Unlike this study, both previous studies did not test large number of cycles to identify its negative impact on oil recovery due to large injected CO₂ volume.

5.2.6. Incremental Increase in Injection Rates

Another test is performed to evaluate incremental injection rates at consecutive cycles in comparison to fixed injection rate. The test includes six different injection scenarios listed in table 5.4, where injection rates are divided on the total number of huff'n'puff cycles with an incremental sequence. Case 1 would represent fixed injection rate scenario. All cases start with the optimum injection rate of 0.025 mm³/d identified during fixed injection rate assessment. Cumulative oil production results in figures 5.29 and 5.30 show that having incremental injection rate at consecutive cycles would result in higher cumulative oil production with an increase by 10% compared to fixed injection rate. Also, higher oil recovery would be achieved with more incremental injection rates cases.

Table 5.4: Different cases of incremental injection rates

Case	Injection Rate (mm ³ /d)					
1	0.025					
2	0.025			0.05		
3	0.025		0.05		0.075	
4	0.025	0.05	0.075		0.1	
5	0.025	0.05	0.075	0.1	0.125	
6	0.025	0.05	0.075	0.1	0.125	0.15

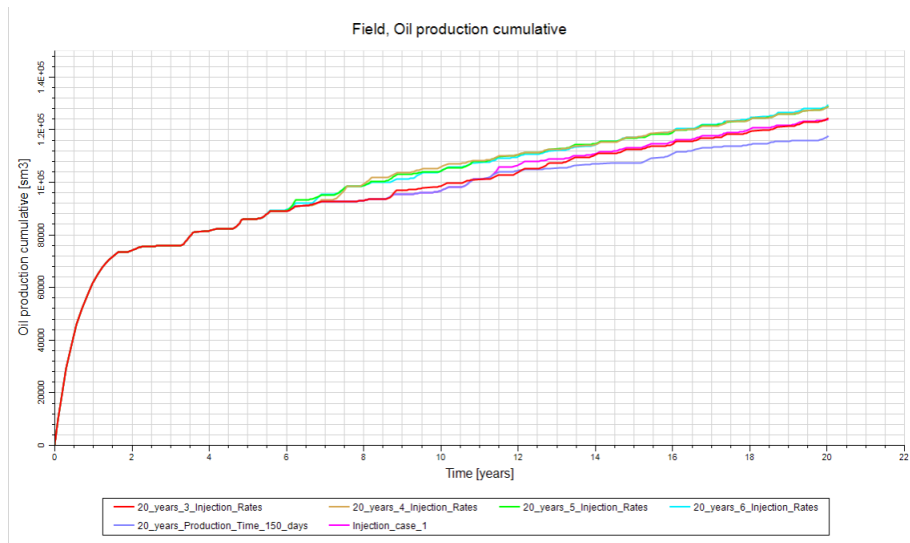


Figure 5.29: Cumulative oil production plots at different incremental injection rate cases

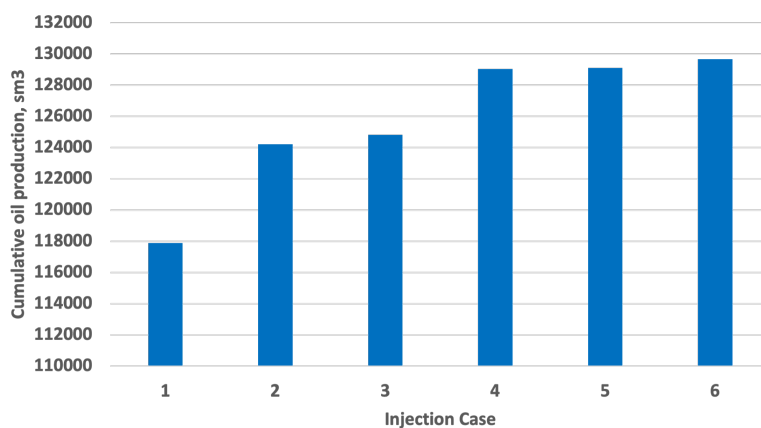


Figure 5.30: Cumulative oil production at different incremental injection rate cases

One aspect that controls oil recovery is pressure support. At a fixed injection rate, reservoir pressure is declining over time due to oil depletion and CO₂ backflow during production as can be observed in figure 5.31. On the other hand, reservoir pressure would increase over time in the case of incremental injection rates. This increase in reservoir pressure due to larger injection rate and volume would lead to higher

dissolution rate as discussed previously. Moreover, it would lead to an increase in advective flow due to pressure gradient in the reservoir leading to a deeper penetration of CO₂ at the later life of EOR. This would be highly beneficial to EOR process as it would manage to produce oil at further areas from the well at a later stage since majority of oil close to the well would be depleted at the early stage leading to higher oil recovery at the end of lifetime. This can be observed through gas saturation distribution comparison between case 1 and 6 at different stages in figure 5.32. Although it holds a great advantage on oil recovery, the use of incremental injection rates would lead to one disadvantage which is higher CO₂ utilization. More CO₂ would need to be injection and handled as well during reproduction. Thus, the optimization in field application of incremental injection rates has to be evaluated based on economic feasibility and CO₂ availability. Nevertheless, this study considers case 6 to be the optimum injection case because it yields the highest oil recovery. This approach of evaluating incremental injection rates at consecutive cycles has not been covered in previous CO₂ EOR numerical studies on tight oil reservoirs.

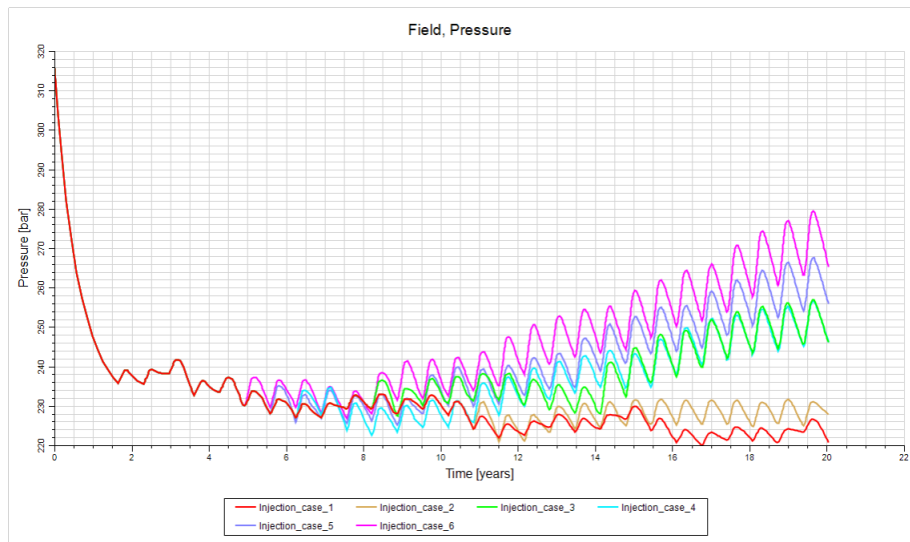


Figure 5.31: Reservoir pressure plots for different incremental injection rate cases

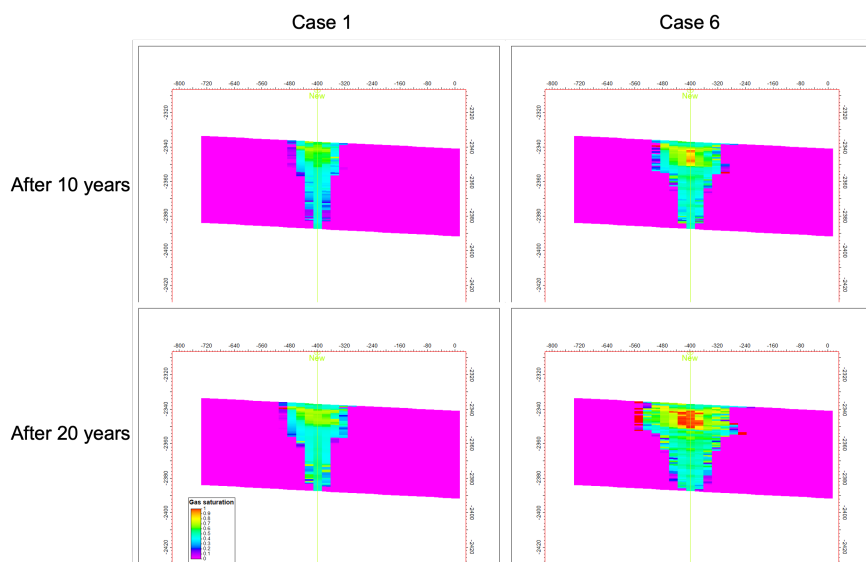


Figure 5.32: Gas saturation cross section map comparison between case 1 and 6

5.2.7. Diffusion Coefficient

A sensitivity test is performed to identify the influence of molecular diffusion mechanism on CO₂ EOR in tight oil reservoir. This is done through running 4 simulation cases with different diffusion coefficients: no diffusion, 0.00432 m²/d, 0.00864 m²/d and 0.0864 m²/d. The modified base case is used with an update including findings from discussed sensitivity studies. Results of cumulative oil production presented in figure 5.33 show that higher diffusion coefficient would result in higher oil recovery. Figure 5.34 shows also the cumulative oil production at the end of project lifetime with the inclusion of cumulative gas production. It indicates that higher diffusion coefficient will not only increase oil recovery, but also reduce CO₂ backflow.

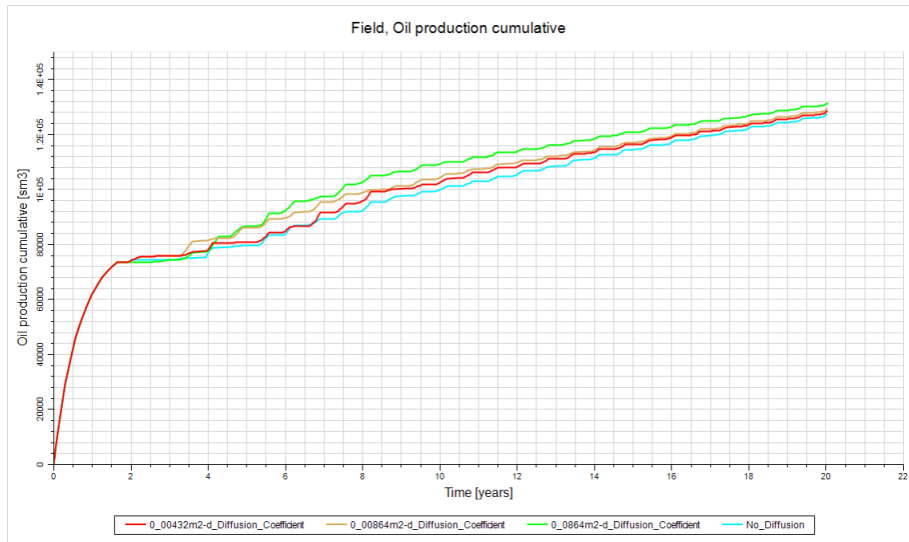


Figure 5.33: Cumulative oil production plots at different diffusion coefficients

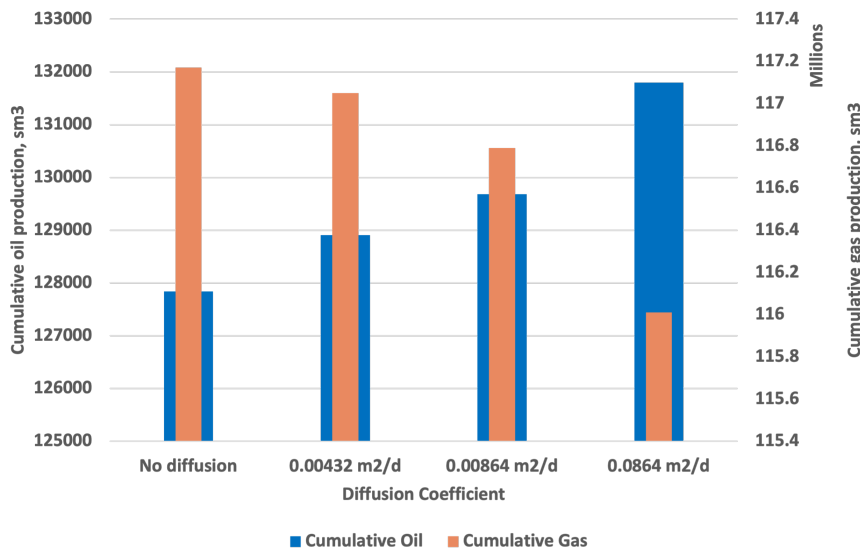


Figure 5.34: Cumulative oil and gas production at different diffusion coefficients

The reason behind the increase in oil recovery and reduction in CO₂ backflow with higher diffusion coefficient is injected CO₂ transport. Higher diffusion coefficient allows injected CO₂ to spread into the reservoir expanding the oil swept area leading to higher oil depletion during production stage. Additionally, the larger movement of injected CO₂ would reduce free gas within the reservoir as it comes into contact with larger

oil volume resulting in larger CO₂ dissolution. This can be observed through gas saturation distribution map in figure 5.35 of different diffusion coefficient cases. These results highlights the significance of molecular diffusion mechanism and the importance of including an accurate estimation of diffusion coefficient in the simulation model for more accurate results.

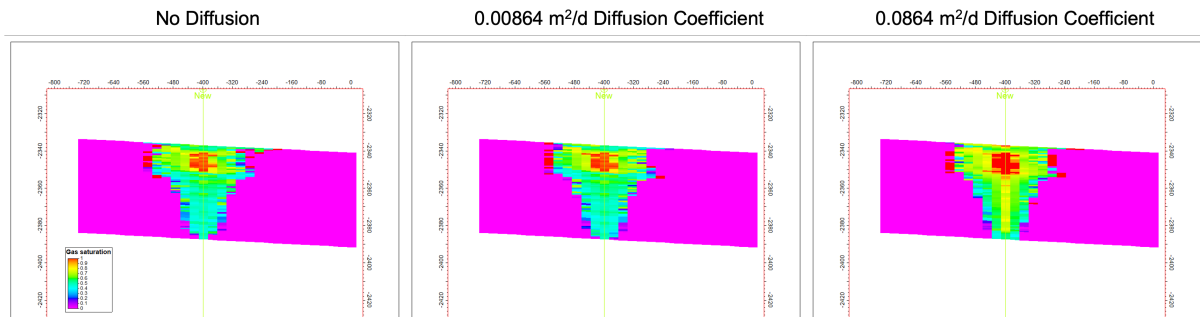


Figure 5.35: Gas saturation cross section map for different diffusion coefficient cases

Comparing the findings with previous work done in the literature, three different studies were conducted on the influence of diffusion coefficient on oil recovery using numerical simulation. Two of those studies reached to a similar conclusion that higher diffusion coefficient would result in higher oil recovery with a maximum tested diffusion coefficient of 0.0864 m²/d similar to this study [12][23]. The third study reached to the same conclusion as well with a maximum tested diffusion coefficient of 0.00432 m²/d [39].

5.2.8. Well Completion

Final test is performed to identify the influence of well completion on CO₂ EOR performance in tight oil reservoir using huff'n'puff scheme. Six different well completion and completion cases listed in table 5.5 are evaluated using optimum input parameters based on previous findings. Results of cumulative oil production in figures 5.36 and 5.37 show that the last case yields the highest oil recovery with 200 m horizontal well completion targeting high permeability layer. The last case shows an increase in cumulative oil production by 1% compared to first case.

Table 5.5: Different cases of well completion

Case	Well Geometry	Well Completion
1	Vertical	All layers perforated (50 m)
2	Vertical	Top layers perforated (25 m)
3	Vertical	Bottom layers perforated (25 m)
4	Horizontal	Perforated 100 m
5	Horizontal	Perforated 200 m
6	Horizontal	Perforated 200 m (High perm)

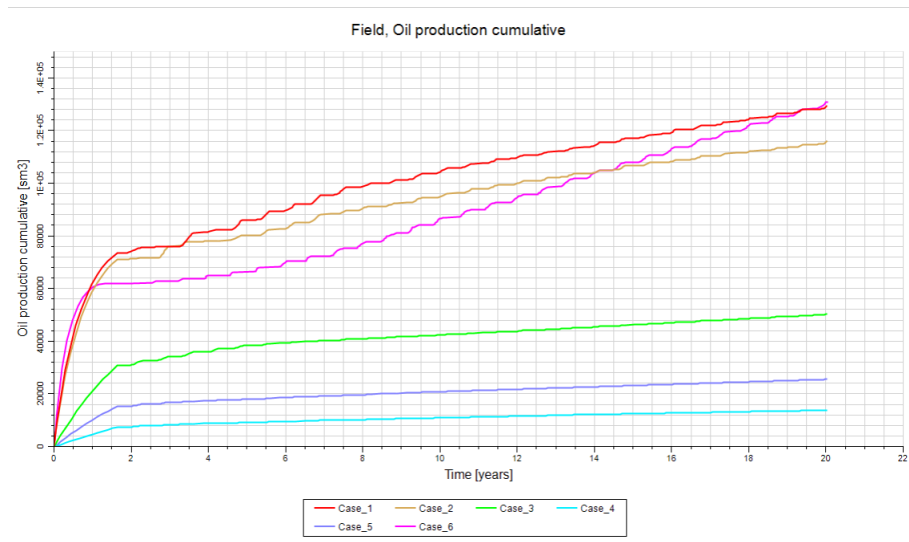


Figure 5.36: Cumulative oil production plots at different well completion cases

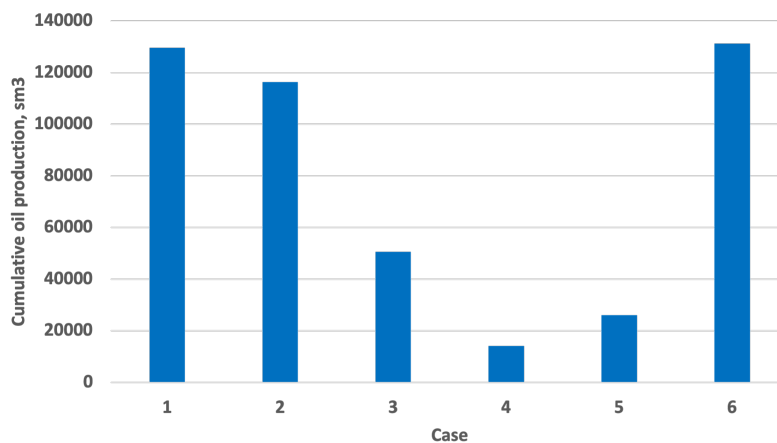


Figure 5.37: Cumulative oil production at different well completion cases

Firstly, the first 3 cases with vertical well completion are evaluated. The difference between those cases is the targeted layer and completion interval. Based on the results, having a high length of perforation across multiple layers would result in higher oil recovery compared to targeting selective layers with shorter completion interval. This is because a larger contact reservoir area would result in a higher well injectivity and larger CO₂ contact volume with the reservoir oil. Cumulative gas injection in figure 5.38 shows that case 3 with selective perforation and limited reservoir contact could not achieve the target CO₂ injection volume compared to the first two cases because of the shorter interval in low permeability section. This led to reaching injection pressure constraint and shutting-off CO₂ injection at later stages. As for case 2, it meets injectivity target similar to case 1 but it still produces less due to lower contact area with the reservoir.

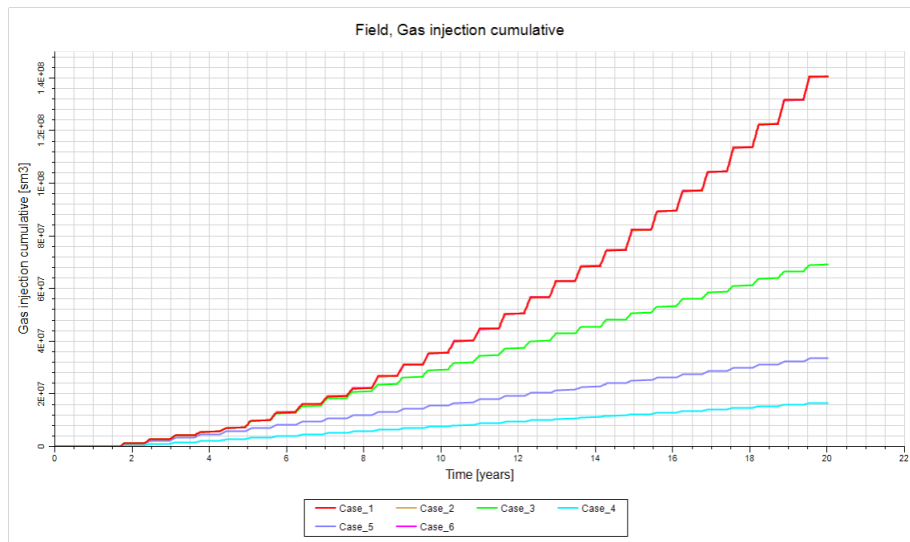


Figure 5.38: Cumulative gas injection plots at different well completion cases

After that, the last 3 cases with horizontal well completion are evaluated. When looking at cases 4 and 5, the only difference is well length since they are both targeting the same layer. Therefore, higher well length would result in higher cumulative oil production. The reason is that it offers larger reservoir contact area leading to higher well injectivity as shown in figure 5.38, where it is similar to cases 1 and 2. When the same well length is targeting a higher permeability layer as in case 6, much higher oil recovery is achieved. This is because of the major well injectivity improvement due to formation permeability. Therefore, it can be concluded that a horizontal well with higher well length targeting a higher permeability layer would yield the highest oil recovery. A horizontal well will outperform the vertical well in the case of targeting a higher permeability layer. The model does not account for permeability difference in the vertical direction, which can restrict injectivity in the case of a k_v/k_h lower than 1. Therefore, it would be recommended to further study the horizontal well performance with various k_v/k_h values and compare it with vertical well performance.

In terms of sweep efficiency, horizontal sweep is relatively good in all cases due to relatively similar reservoir petrophysical properties in the geological model. On the other hand, the model accounts for high petrophysical properties' variations vertically since the model is divided into 62 different layers within a 50 m thickness. Figure 5.39 shows a cross section of gas saturation distribution at the end of CO₂ EOR for all cases. A low vertical sweep efficiency is observed in first and second cases with higher sweep in upper layers. On the other hand, case 3 with bottom perforation shows a good vertical sweep across reservoir thickness. This can be attributed to the effect of buoyancy force that leads to the upward movement of injected CO₂. This is also observed in the horizontal completion cases. It can be concluded that targeting bottom layers in horizontal or vertical well completion will improve vertical sweep efficiency.

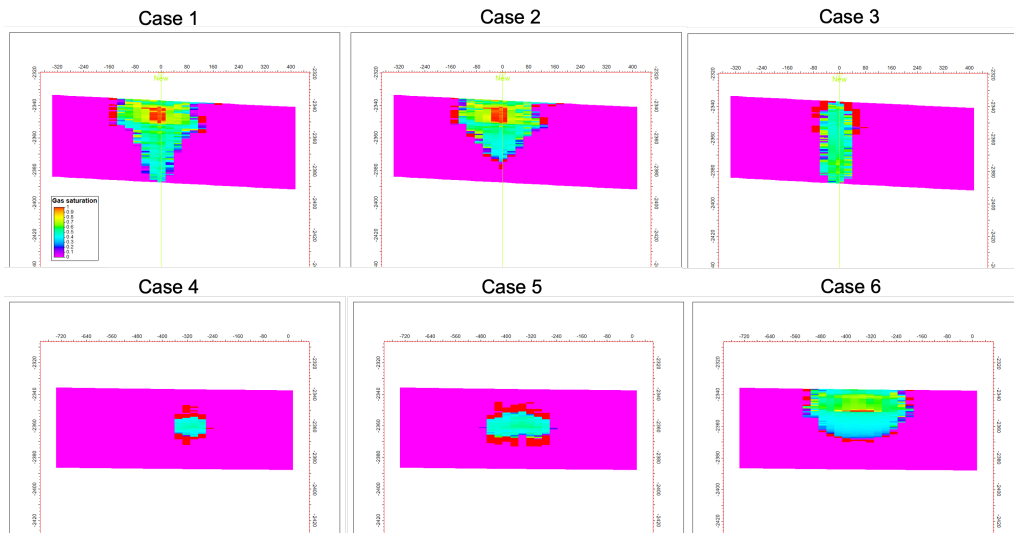


Figure 5.39: Gas saturation cross section map of different well completion cases

Lastly, it is worth noting that all these cases will have different oil production performance during the primary recovery stage. This can be observed in figure 5.40 showing oil production rate for the different cases during primary recovery stage. Thus, each case would need a separate assessment of primary recovery period and starting time for CO₂ EOR to achieve the highest oil recovery. Nevertheless, the conclusions from the well completion evaluation still stands without the need to perform individual changes on CO₂ EOR period.

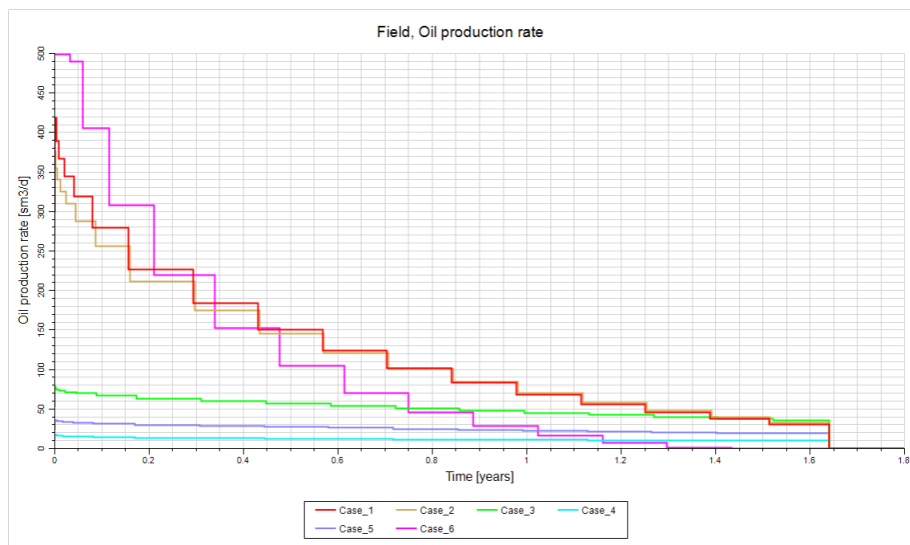


Figure 5.40: Oil production rates at different well completion cases during primary recovery

5.3. Optimum Case

Based on the findings and conclusions from the performed sensitivity study, an optimum CO₂ EOR huff'n'puff case is designed. The parameters used for this optimum case are presented in table 5.6. As for injection strategy, it is listed in table 5.7 showing a detailed sequence of injection rates following incremental injection rate approach. In this case, a horizontal well completion is chosen with 200 m length. Simulation results of the optimum case are illustrated in figure 5.41. Unlike the base case, optimum case results show a maintained reservoir pressure across project lifetime after primary depletion period. In addition,

higher oil recovery is observed at later life indicating the potential of the optimum case to continue for a longer lifetime. The modifications made during the sensitivity study managed to enhance cumulative oil production by 32% from the initially set base case. This highlights the significance of different controlled parameters on CO₂ EOR huff'n'puff oil recovery.

Table 5.6: Model parameters for optimum case

Parameter	Value
Lifetime, years	20
Production bottomhole pressure constraint, bars	100
Injection time per cycle, days	60
Soaking time per cycle, days	30
Production time per cycle, days	150
Number of cycles	29
Well length, m	200

Table 5.7: Injection rates sequence

Step	Injection rate, mm ³ /d	Number of Cycle
1	0.025	6
2	0.05	5
3	0.075	5
4	0.1	5
5	0.125	4
6	0.15	4

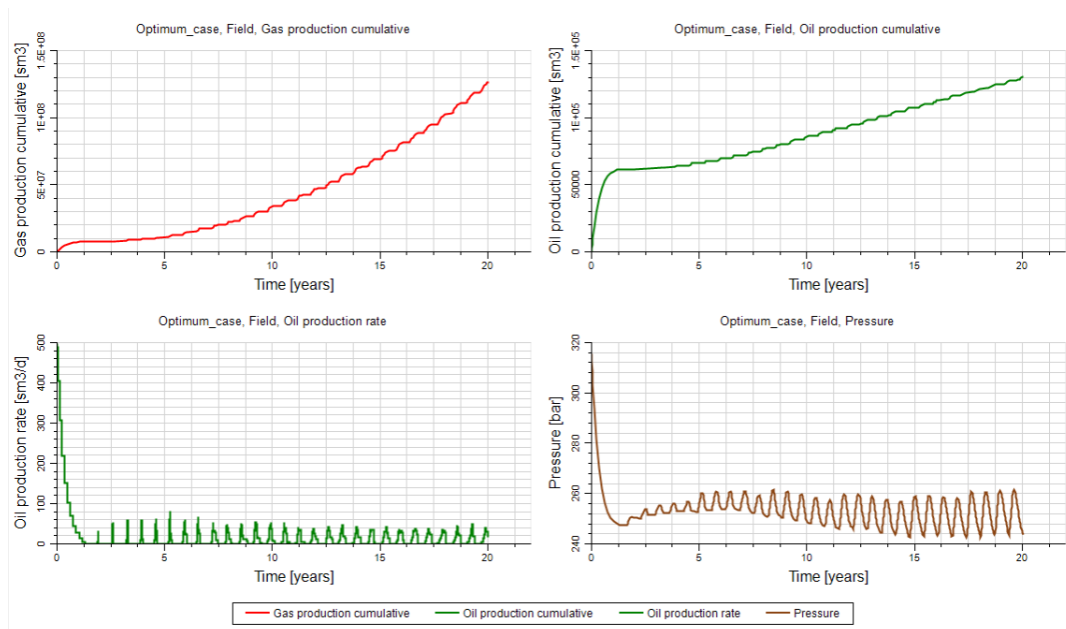


Figure 5.41: Simulation results of optimum case

6

Conclusions

In this thesis, a comprehensive assessment has been conducted on CO₂ EOR performance in unconventional oil reservoir using huff'n'puff scheme. Numerical simulation has been used to perform the assessment utilizing a sector model from an open-source geological model. A sensitivity study conducted on several parameters to determine their impact on cumulative oil production in unconventional oil reservoir. The main conclusions drawn from this thesis are as follows:

- 1) The best strategy to develop an unconventional oil reservoir using CO₂ huff'n'puff is by including a primary recovery period utilizing reservoir driven pressure. Results showed that after including a primary recovery period of 2 years, an increase of 15% in cumulative oil production is realized compared to the case where CO₂ huff'n'puff started from the beginning. The duration of the primary recovery period would be dependent on reservoir conditions such as reservoir pressure and fluid properties.
- 2) The conducted Sensitivity study on previously studied CO₂ huff'n'puff parameters in the literature verified their findings in terms of their influence on oil production. This work extends beyond sharing the results and comparison with previous studies, but also provides its own interpretation and evaluation leading to these results.
- 3) The implementation of incremental injection rates in subsequent cycles as a CO₂ injection scheme in huff'n'puff method instead of fixed injection rate improved cumulative oil production. Results showed that cumulative oil production becomes 10% higher when incremental injection scheme is followed due to higher pressure support after oil and CO₂ depletion after each cycle. This strategy is aiming to maintain reservoir pressure and allow for deeper penetration of injected CO₂ for larger oil sweep volume.
- 4) A new approach is used to evaluate injection time impact on oil production by maintaining a fixed CO₂ injection in each cycle through changing injection rate. Increasing injection period by 10 times in each cycle with a fixed injected CO₂ volume of 3.75 mm³ per cycle improved cumulative oil production by 7%. This is a result of longer diffusion and dissolution time given eventhough injection rate and pressure is lower.
- 5) The evaluation of different well completions and geometries indicated that bottom CO₂ injection by targeting bottom layers improves vertical sweep efficiency. This is attributed to the effect of buoyancy forces due to the difference in densities between injected CO₂ and reservoir fluids.

Recommendations

This chapter provides a brief overview of the primary recommendations for the future continuation of this research project.

- 1) The study focuses on CO₂ EOR performance from oil production aspect. Nevertheless, it would be recommended to include the impact of each scenario on CO₂ utilization and storage for a comprehensive evaluation.
- 2) The used geological model has certain boundary conditions that can influence simulation results when a different geological model is used. Therefore, it is recommended to include petrophysical changes such as presence of fractures, mineral dissolution and asphaltene precipitation that can occur due to CO₂ injection in the reservoir simulation. Simulation results after implementing these petrophysical changes can be used to compared the findings of this thesis work.
- 3) This study uses a light oil composition for the evaluation of CO₂ EOR in unconventional reservoir with no other mobile fluids present. It would be recommended to perform this study with different oil composition in addition to the inclusion of other mobile fluids such as water aquifer or gas cap. This is to evaluate the influence of other mobile fluids present on oil recovery and to confirm findings and share differences.

References

- [1] Narendra Kumar et al. "Fundamental aspects, mechanisms and emerging possibilities of CO₂ miscible flooding in Enhanced Oil Recovery: A Review". In: *Fuel* 330 (2022), p. 125633. DOI: 10.1016/j.fuel.2022.125633.
- [2] Nidhal Badrouchi et al. "Evaluation of CO₂ enhanced oil recovery in unconventional reservoirs: Experimental parametric study in the Bakken". In: *Fuel* 312 (2021), p. 122941. DOI: 10.1016/j.fuel.2021.122941.
- [3] Dheiaa Alfarge et al. "CO₂-EOR mechanisms in huff-n-puff operations in shale oil reservoirs based on history matching results". In: *Fuel* 226 (2018), pp. 112–120. DOI: 10.1016/j.fuel.2018.04.012.
- [4] Dheiaa Alfarge et al. "Analysis of IOR pilots in Bakken Formation by using numerical simulation". In: (2017). DOI: 10.2118/188633-ms.
- [5] Wei-Yu Tang et al. "Further discussion of CO₂ Huff-n-puff mechanisms in tight oil reservoirs based on NMR monitored fluids spatial distributions". In: *Petroleum Science* 20.1 (2022), pp. 350–361. DOI: 10.1016/j.petsci.2022.08.014.
- [6] Haiyang Yu et al. "Experimental study on EOR performance of CO₂-based flooding methods on tight oil". In: *Fuel* 290 (2021), p. 119988. DOI: 10.1016/j.fuel.2020.119988.
- [7] Xiang Zhou et al. "Performance evaluation of CO₂ flooding process in tight oil reservoir via experimental and Numerical Simulation Studies". In: *Fuel* 236 (2018), pp. 730–746. DOI: 10.1016/j.fuel.2018.09.035.
- [8] Xiang Li et al. "Experimental study of oil recovery from pore of different sizes in tight sandstone reservoirs during CO₂ flooding". In: *Journal of Petroleum Science and Engineering* 208 (2021), p. 109740. DOI: 10.1016/j.petro1.2021.109740.
- [9] Maolei Cui et al. "Characteristics of water alternating CO₂ injection in low-permeability beach-bar sand reservoirs". In: *Energy Geoscience* (2022), p. 100119. DOI: 10.1016/j.engeos.2022.06.007.
- [10] Dazhong Ren et al. "Feasibility evaluation of CO₂ EOR and storage in tight oil reservoirs: A demonstration project in the Ordos Basin". In: *Fuel* 331 (2022), p. 125652. DOI: 10.1016/j.fuel.2022.125652.
- [11] Zheng Chen et al. "Characteristics and mechanisms of supercritical CO₂ flooding under different factors in low-permeability reservoirs". In: *Petroleum Science* 19.3 (2022), pp. 1174–1184. DOI: 10.1016/j.petsci.2022.01.016.
- [12] Wei Yu et al. "CO₂ injection for enhanced oil recovery in Bakken tight oil reservoirs". In: *Fuel* 159 (2015), pp. 354–363. DOI: 10.1016/j.fuel.2015.06.092.
- [13] Bing Kong et al. "Simulation and optimization of CO₂ Huff-and-puff processes in tight oil reservoirs". In: (2016). DOI: 10.2118/179668-ms.
- [14] Nidhal Badrouchi et al. "Experimental investigation of CO₂ injection side effects on reservoir properties in Ultra Tight Formations". In: *Journal of Petroleum Science and Engineering* 215 (2022), p. 110605. DOI: 10.1016/j.petro1.2022.110605.
- [15] Kaiqiang Zhang et al. "A review of experimental methods for determining the oil-gas minimum miscibility pressures". In: *Journal of Petroleum Science and Engineering* 183 (2019), p. 106366. DOI: 10.1016/j.petro1.2019.106366.
- [16] Huang Feng et al. "Assessment of miscibility effect for CO₂ flooding EOR in a low permeability reservoir". In: *Journal of Petroleum Science and Engineering* 145 (2016), pp. 328–335. DOI: 10.1016/j.petro1.2016.05.040.

- [17] Meng Cao et al. "Oil recovery mechanisms and asphaltene precipitation phenomenon in immiscible and miscible CO₂ flooding processes". In: *Fuel* 109 (2013), pp. 157–166. DOI: 10.1016/j.fuel.2013.01.018.
- [18] Fenglan Zhao et al. "Performance and applicable limits of multi-stage gas channeling control system for CO₂ flooding in ultra-low Permeability Reservoirs". In: *Journal of Petroleum Science and Engineering* 192 (2020), p. 107336. DOI: 10.1016/j.petrol.2020.107336.
- [19] Chen Xiaolong et al. "Effect of gravity segregation on CO₂ flooding under various pressure conditions: Application to CO₂ sequestration and oil production". In: *Energy* 226 (2021), p. 120294. DOI: 10.1016/j.energy.2021.120294.
- [20] Dheiaa Alfarge et al. "Feasibility of CO₂-EOR in shale-oil reservoirs: Numerical Simulation Study and Pilot tests". In: (2017). DOI: 10.7122/485111-ms.
- [21] Mohamed Gamal Rezk et al. "Uncertainty effect of CO₂ molecular diffusion on oil recovery and gas storage in underground formations". In: *Fuel* 324 (2022), p. 124770. DOI: 10.1016/j.fuel.2022.124770.
- [22] Jinhua Ma et al. "Enhanced Light Oil Recovery from tight formations through CO₂ Huff 'n' Puff Processes". In: *Fuel* 154 (2015), pp. 35–44. DOI: 10.1016/j.fuel.2015.03.029.
- [23] B. Sennaoui et al. "Reservoir simulation study and optimizations of CO₂ Huff-n-puff mechanisms in Three forks formation". In: (2022). DOI: 10.56952/igs-2022-137.
- [24] Figuera Luis et al. "Case study of CO₂ injection to enhance oil recovery into the transition zone of a tight carbonate reservoir". In: (2016). DOI: 10.2118/183203-ms.
- [25] Huan Peng et al. "Influence of Supercritical CO₂ on the physical property of Tight Sandstone". In: *Petroleum* (2022). DOI: 10.1016/j.petlm.2022.10.003.
- [26] Jingchen Ding et al. "Supercritical CO₂ sequestration and enhanced gas recovery in tight gas reservoirs: Feasibility and factors that influence efficiency". In: *International Journal of Greenhouse Gas Control* 105 (2020), p. 103234. DOI: 10.1016/j.ijggc.2020.103234.
- [27] Nidhal Badrouchi et al. "Experimental investigation of CO₂ injection side effects on reservoir properties in Ultra Tight Formations". In: *Journal of Petroleum Science and Engineering* 215 (2022), p. 110605. DOI: 10.1016/j.petrol.2022.110605.
- [28] Zhou YUAN et al. "The effect of inorganic salt precipitation on oil recovery during CO₂ flooding: A case study of chang 8 block in Changqing oilfield, NW China". In: *Petroleum Exploration and Development* 48.2 (2021), pp. 442–449. DOI: 10.1016/s1876-3804(21)60035-6.
- [29] Yuting Dai et al. "Evaluation of the impact of CO₂ Geological Storage on tight oil reservoir properties". In: *Journal of Petroleum Science and Engineering* 212 (2022), p. 110307. DOI: 10.1016/j.petrol.2022.110307.
- [30] Kai Zhang et al. "A way to improve water alternating gas performance in tight oil reservoirs". In: (2016). DOI: 10.2118/180858-ms.
- [31] Zhaojie Song et al. "A critical review of CO₂ enhanced oil recovery in tight oil reservoirs of North America and China". In: *Fuel* 276 (2020), p. 118006. DOI: 10.1016/j.fuel.2020.118006.
- [32] Reem Ali Mabkhout AlSeiari et al. "A success story of the first miscible CO₂ Wag Miscible Wag pilots in a giant carbonate reservoir in Abu Dhabi". In: (2022). DOI: 10.2118/211456-ms.
- [33] Xing Huang et al. "Asphaltene Precipitation and reservoir damage characteristics of CO₂ flooding in different microscopic structure types in tight light oil reservoirs". In: *Fuel* 312 (2021), p. 122943. DOI: 10.1016/j.fuel.2021.122943.
- [34] Jorge Costa Gomes. "An Open Access Carbonate Reservoir Model". PhD thesis. Mar. 2022. DOI: 10.13140/RG.2.2.20631.65445/1.
- [35] Michel Rebelle et al. "Integrated Reservoir Characterization of an Upper Kharaib carbonate reservoir from onshore Abu Dhabi (UAE)". In: (2012). DOI: 10.2118/161190-ms.

- [36] Xiangji Dou et al. "The study of CO₂ flooding and sequestration in tight gas reservoir: Different completion measures". In: (2015). DOI: 10.2118/178287-ms.
- [37] Schlumberger. *ECLIPSE Reservoir Engineering Software*. 2021.
- [38] Schlumberger. *Petrel Seismic-to-Evaluation Software*. 2021.
- [39] Yuan Zhang et al. "Simulation study of factors affecting CO₂ Huff-N-puff process in tight oil reservoirs". In: *Journal of Petroleum Science and Engineering* 163 (2018), pp. 264–269. DOI: 10.1016/j.petrol.2017.12.075.
- [40] Hutthapong Yoosook et al. "CO₂ utilization for enhance oil recovery with huff-N-puff process in depleting heterogeneous reservoir". In: *Energy Procedia* 141 (2017), pp. 184–188. DOI: 10.1016/j.egypro.2017.11.035.
- [41] Yong Tang et al. "Numerical simulation and optimization of enhanced oil recovery by the in situ generated co₂huff-n-puff process with compound surfactant". In: *Journal of Chemistry* 2016 (2016), pp. 1–13. DOI: 10.1155/2016/6731848.
- [42] Mengjing Cao et al. "Numerical simulation and performance evaluation of CO₂ Huff-N-puff processes in unconventional oil reservoirs". In: (2017). DOI: 10.7122/486556-ms.
- [43] Samuel Afari et al. "Optimization of CO₂ huff-N-puff eor in the Bakken formation using numerical simulation and response surface methodology". In: *Journal of Petroleum Science and Engineering* 215 (2022), p. 110552. DOI: 10.1016/j.petrol.2022.110552.
- [44] Tarek H. Ahmed. *Reservoir Engineering Handbook*. Gulf Professional Publishing, 2019.
- [45] F. F. Li et al. "An improved method to study CO₂-oil relative permeability under miscible conditions". In: *Journal of Petroleum Exploration and Production Technology* 5.1 (2014), pp. 45–53. DOI: 10.1007/s13202-014-0122-1.
- [46] M.M. Honarpour et al. "Chapter 8 permeability and relative permeability of carbonate reservoirs". In: *Developments in Petroleum Science* (1992), pp. 399–416. DOI: 10.1016/s0376-7361(09)70131-1.
- [47] Xiaoliang Huang et al. "Functions of capillary pressure and dissolution in the CO₂-flooding process in low-permeability reservoirs". In: *Journal of Petroleum Exploration and Production Technology* 10.5 (2020), pp. 1881–1890. DOI: 10.1007/s13202-020-00853-0.
- [48] Zhengdong Lei et al. "Simulation and optimization of CO₂ Huff-N-puff processes in tight oil reservoir: A case study of chang-7 tight oil reservoirs in Ordos Basin". In: (2018). DOI: 10.2118/191873-ms.